AD 680275

AD

USAAVLABS TECHNICAL REPORT 68-62

FABRICATION AND FUNCTIONAL TEST OF A FLIGHTWORTHY FLUIDIC YAW DAMPER

By

Walter M. Posingies

October 1968

U. S. ARMY AVIATION MATERIEL LABORATORIES FORT EUSTIS, VIRGINIA

CONTRACT DAAJ02-67-C-0056
HONEYWELL INC.
AEROSPACE DIVISION
MINNEAPOLIS, MINNESOTA

This document has been approved for public release and sale; its distribution is unlimited.

64

DEPARTMENT OF THE ARMY
U. S. ARMY AVIATION MATERIEL LABORATORIES
FORT EUSTIS, VIRGINIA 23604

This report has been reviewed by the U. S. Army Aviation Materiel Laboratories and is considered to be technically sound. The report is published for the exchange of information and the stimulation of ideas.

Task IF121401A14186

Contract DAAJ02-67-C-0056

USAAVLABS Technical Report 68-62

October 1968

FABRICATION AND FUNCTIONAL TEST OF A FLIGHTWORTHY FLUIDIC YAW DAMPER

Final Report
Honeywell Document 20885-FR1

by
Walter M. Posingies

Prepared by

Honeywell Inc.
Aerospace Division
Minneapolis, Minnesota

for

U. S. ARMY AVIATION MATERIEL LABORATORIES
FORT EUSTIS, VIRGINIA

SUMMARY

The objective of this program was to design, fabricate, and perform acceptance tests on a flightworthy fluidic yaw damper system and to provide support to the Bell Helicopter Company during flight evaluation of the system. Control-system characteristics were optimized for the UH-1 series helicopters.

This program incorporated significant improvements in the areas of component design, high-pass circuit simplification, noise reduction, and fabrication techniques. Temperature compensation studies illustrated a technique for maintaining a relatively constant rate-sensor scale factor over a wide range of fluid temperatures.

Flightworthiness testing demonstrated that the system provided the required transfer function and was suitable for flight test.

The flight test (not reported in this document) confirmed that the system was suitable for the helicopter environments and that it would increase the vehicle directional damping ratio from 0.3 to 0.6.

Post-flight tests in the laboratory determined the bench performance of the system under several special conditions to which the system had been adjusted during the flight test.

This program demonstrated that fluidic systems operating with hydraulic fluid can accurately provide simple control functions. Consistent and trouble-free performance obtained during this development indicates that fluidic systems should be considered for applications which require similar functions.

FOREWORD

This document concludes a research and development program by the U.S. Army Aviation Materiel Laboratories under Contract DAAJ02-67-C-0056. The technical monitor for this program is Mr. G. W. Fosdick. The author of the appendix to this report is Mr. D. D. Bengston.

This is the third in a series of contracts aimed at demonstrating the feasibility of using hydraulically operated fluidic devices to augment the stability of helicopters. The objective is to design and flight test a flightworthy hydrofluidic yaw damper optimized to the requirements established in previous programs. The work presented in this report was initiated 28 June 1967 and completed 28 April 1968.

The first program, Contract DA 44-177-AMC-294(T), established the requirements for a yaw damper compatible with the UH-1 series helicopters. This contract also demonstrated the feasibility of hydraulic fluidics providing the functions necessary for short-period stability augmentation for the helicopter. The program, completed in 1966, is described in USAAVLABS Technical Report 66-87, Fluid State Hydraulic Damper, February 1967.

A second program, Contract DAAJ02-67-0003, demonstrated the high reliability of hydraulic fluidic devices. Sixteen of each of the basic components used in a damper system (rate sensor, trim valve, bellows, and proportional amplifier) were subjected to 3000 hours of operation under various environments. No failures were experienced in this program, where each component type received about 50,000 hours of reliability testing. Details of this program are presented in USAAVLABS Technical Report 68-36, Fluidic Reliability, June 1968.

The Servo Schematic is reprinted with the permission of the Hydraulic Research and Manufacturing Co., Burbank, California.

TABLE OF CONTENTS

		Page
	SUMMARY	iii
	FOREWORD	v
	LIST OF ILLUSTRATIONS	ix
	LIST OF TABLES	xi
	LIST OF SYMBOLS	xii
SECTION I	INTRODUCTION	1
SECTION II	SYSTEM DESIGN	2
	Background	2
	Design Requirements	2
	Circuit Selection	4
SECTION III	MECHANIZATION OR COMPONENT DESIGN	7
	General	7
	Rate Sensor	7
	Amplifiers	9
	Capacitors	9
	Restrictors	9
	Manifold Plate	12
	Transducers	12
SECTION IV	HYDRAULIC POWER SUPPLY	14
	General	14
	Hydraulic Power Pack	14
	Heat Exchanger	14
	Valves - Gain Changing	16
	Oil-Level Indicator	16
SECTION V	SYSTEM TEST RESULTS	18
	High-Pass Time Constant	18
	Frequency Response	18
	Effects of Temperature and Flow	22
	Rate Sensor Temperature Compensation	24
	Effects of Transducers on System Performance	28
	Filter Capacitor	28
SECTION VI	ACCEPTANCE TESTS	29

TABLE OF CONTENTS (CONCLUDED)

		Page
SECTION VII	POST-FLIGHT TESTS	35
	Objectives	35
	Hard-over Problems	35
	Flight-Test Conditions	35
	System Test Results	37
	Temperature Compensation Test Results	37
SECTION VIII	CONCLUSIONS	43
SECTION IX	RECOMMENDATIONS	44
APPENDIX	PREFLIGHT ACCEPTANCE TEST REPORT	45
	Abstract	45
	Unit Tested	45
	Reference Documents	45
	Procedure and Results	45
DISTRIBUTION		52

LIST OF ILLUSTRATIONS

Figure		Page
1	System Response Requirements	3
2	High-Pass Circuit Used in Feasibility Program	5
3	Flight System Circuit Diagram	6
4	Fluidic Yaw Damper Flight Test Package	8
5	Preamplifier Gain Curve	10
6	Power Amplifier Gain Curve	11
7	Manifold Plate	13
8	Hydraulic Power Supply	15
9	Reservoir Calibration	17
10	System Step Response	19
11	System Frequency Response (Large Amplitude)	20
12	System Frequency Response (Small Amplitude)	21
13	Preliminary Data on Gain as a Function of Temperature	23
14	Rate Sensor Schematic	25
15	Primary Sink Flow Versus Temperature	26
16	Sensor Gain Versus Temperature	27
17	Acceptance Test Setup	30
18	Computer Simulation	31
19	Closed-Loop Step Response at 60 Knots	32
20	Closed-Loop Step Response at 90 Knots	33
21	Closed-Loop Step Response at 120 Knots	34
22	Servo Schematic	36

Figure		Page

Figure		Page
23	Post-Flight Test Amplitude Response	38
24	Post-Flight Test Phase Response	39
25	Effect of Compensation on Flight Test Rate Sensor	40
26	Effect of Compensation on Flight Test System	42

LIST OF TABLES

Table		Page
I	Effects of Transducers on System Response	28
II	Simulated System Performance With and Without Fluidic Control	29
III	Failure Criteria	46
IV	Initial Performance Test	46
V	Vibration Performance	47
VI	Post-Vibration Performance Test	48
VII	+20°F Ambient Environmental Performance Test	48
VIII	+100°F Environmental Performance Test	49
IX	Post-Environmental Performance Test	49
X	Closed-Loop Response	51

LIST OF SYMBOLS

ΔP - differential pressure

gpm - gallons per minute

deg - degree

sec - second

psig - pounds per square inch gage

in. - inch

lb - pound

dia - diameter

R - resistance $\frac{\text{lb sec}}{\text{in.}^5}$

R.C. - resistance capacitance time constant

°F - degree Fahrenheit

% - percent

cps - cycles per second

g - acceleration due to gravity (in./sec^2)

min - minute

θ_T - tail rotor angle (deg)

β - sideslip angle (deg)

ζ - damping ratio

C - capacitance (in.^{5}/lb)

S - Laplace operator (1/sec)

T - time constant (sec)

a	-	$1/T$ (sec^{-1})
P_s	-	supply pressure
P_a	-	amplifier supply pressure
ϕ	-	roll angle deg
db	-	decibel (20 times log of gain)
tdr	-	transducer
$\dot{\psi}$	-	yaw rate (deg per sec)
ψ	-	yaw heading (deg)
Ω	-	fluidic ohms $\frac{\text{lb sec}}{\text{in.}^5}$

BLANK PAGE

SECTION I

INTRODUCTION

This report describes the research and development work accomplished in designing, fabricating, and evaluating a flightworthy hydraulic fluidic yaw damper. Included in this report are design requirements, a description of the mechanization used and the reasons for its selection, the development test results, and a definition of system performance both before and after the flight test.

SECTION II

SYSTEM DESIGN

BACKGROUND

A feasibility program for a fluid-state hydraulic damper [Contract DA 44-177-AMC-294(T)] established a required transfer function for use with the yaw axis of the UH-1 series helicopters. These requirements are shown in Figure 1 for a system operating with the specified actuator and linkage gain.

Hardware developed in the previous program demonstrated the feasibility of providing the required transfer function and the need for specific improvements,which became design objectives for this follow-on program.

DESIGN REQUIREMENTS

The objectives of this program were to build a flightworthy damper system with a transfer function as shown in Figure 1 and to incorporate design improvements in the following areas:

1. Reduced sensitivity to oil viscosity changes
2. Gain adjustment capability
3. Pilot trim and servo disengage switching
4. System noise reduction
5. Packaging

Other design requirements were to provide:

1. An electric-motor-driven, self-contained, low-pressure hydraulic power pack to supply the low-pressure portions of the fluidic system
2. Instrumentation necessary to measure the following data during flight:
    - Rate-sensor flow rate
    - Rate-sensor output ΔP
    - Series servo input ΔP

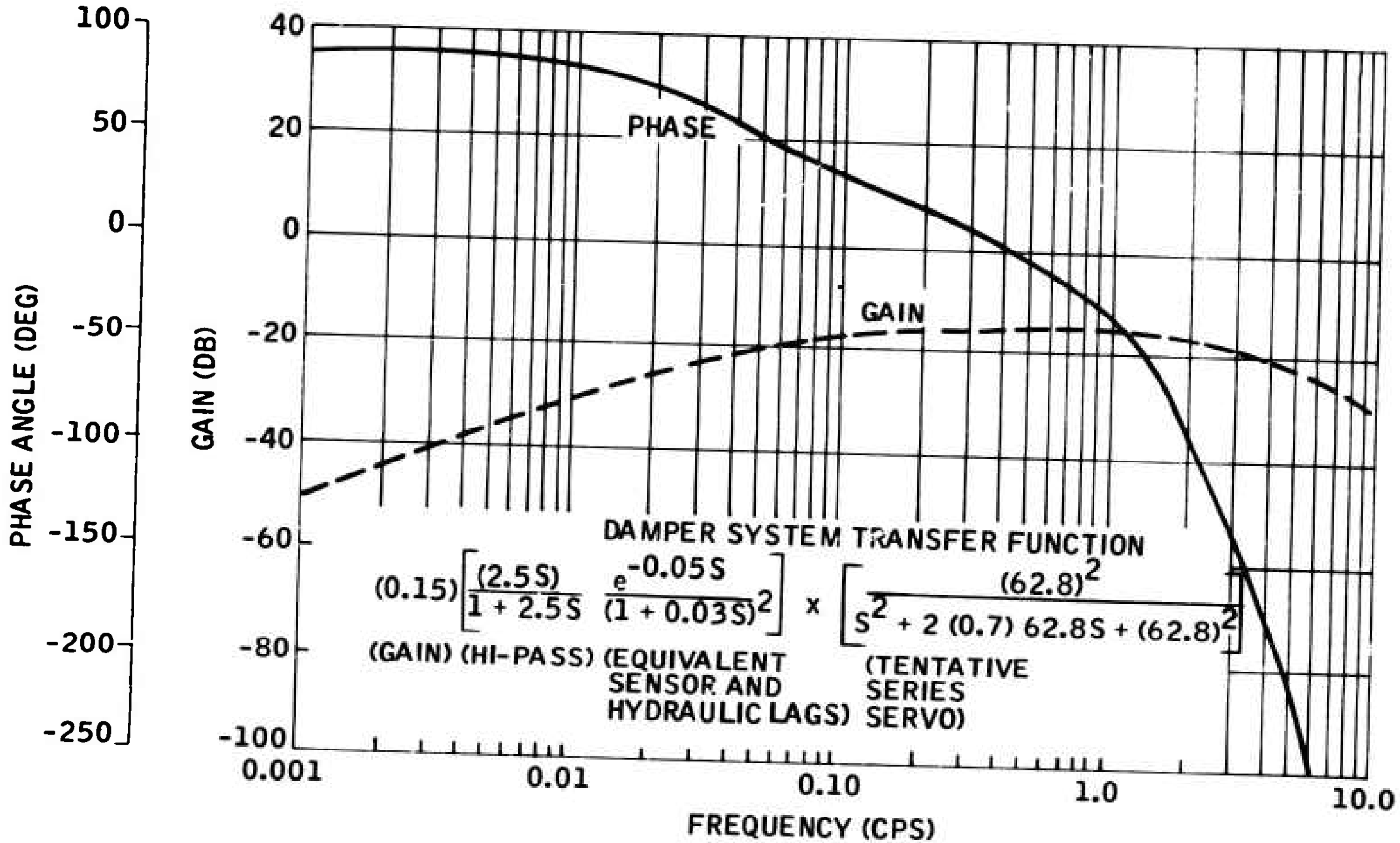

Figure 1. System Response Requirements.

- Fluid system supply pressure
- Fluid system return pressure
- High-pass circuit output ΔP

3. Splash guards to protect the crew in the event of a hydraulic failure

4. A relay which permits the use of remotely located 28-vdc low-current switches to operate the hydraulic pump

CIRCUIT SELECTION

A significant improvement in system performance was obtained by using series capacitors for the high-pass circuit. The previous design (Figure 2) used five amplifiers to provide the same gain and response as the two-amplifier series capacitor network shown in Figure 3.

The previous circuit obtained the high-pass function by subtracting lagged rate from the rate signal; i. e.,

$$1 - \frac{1}{TS+1} = \frac{TS}{TS+1}$$

Gain of the preamplifier in this circuit was low, since it was driving into two amplifiers. Gain of the parallel output amplifiers was also low, since the output impedance of one becomes a load to the other.

The selected circuit (Figure 3) consists of a vortex rate sensor, two bellows (series capacitors), two amplifiers, and an electrical trim valve. Figure 3 also shows the locations of the flight-test transducers.

The series bellows arrangement shown in Figure 3 provides a transfer function with the characteristic of

$$\frac{TS}{TS+1} \quad \text{or} \quad \frac{S}{S+a}$$

The dc gain of this circuit is zero, and the high-frequency gain is 1.0.

Two functions were provided by the trim valve: external electrical signals for trim, calibration, or control may be applied to the system through this interface; and the valve provides a bias flow into each control port of the second-stage amplifier. The level of this flow determines the input impedance of the power amplifier. Signals from the bellows and trim valve are summed at the control ports of the last stage and are amplified.

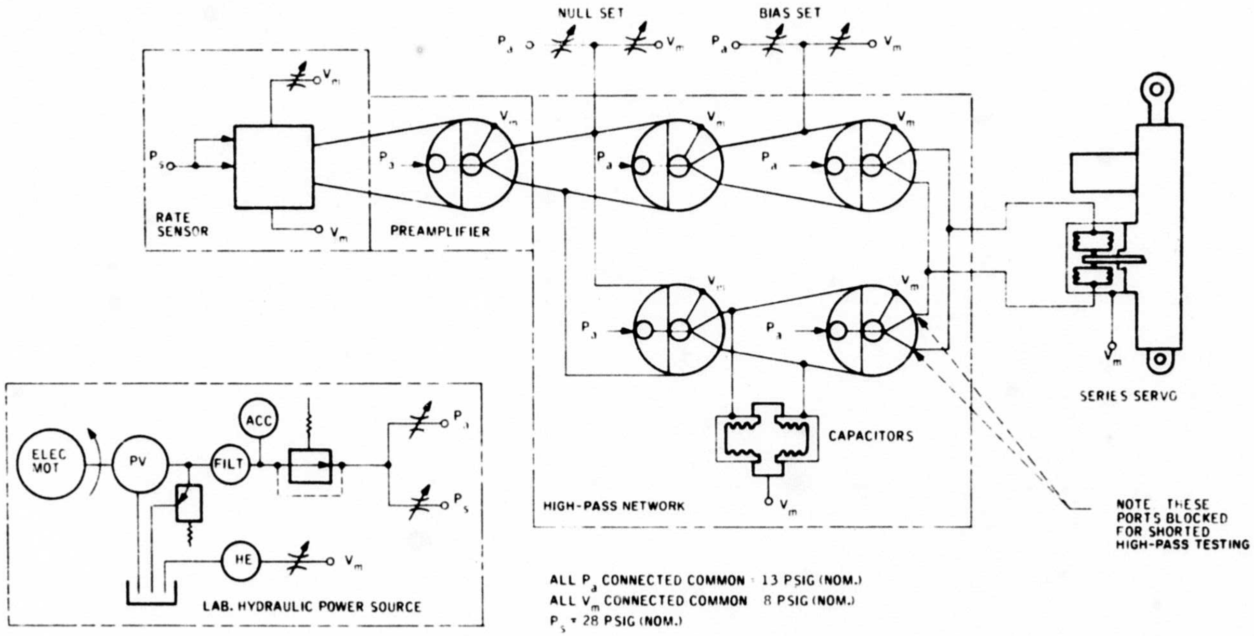

Figure 2. High-Pass Circuit Used in Feasibility Program.

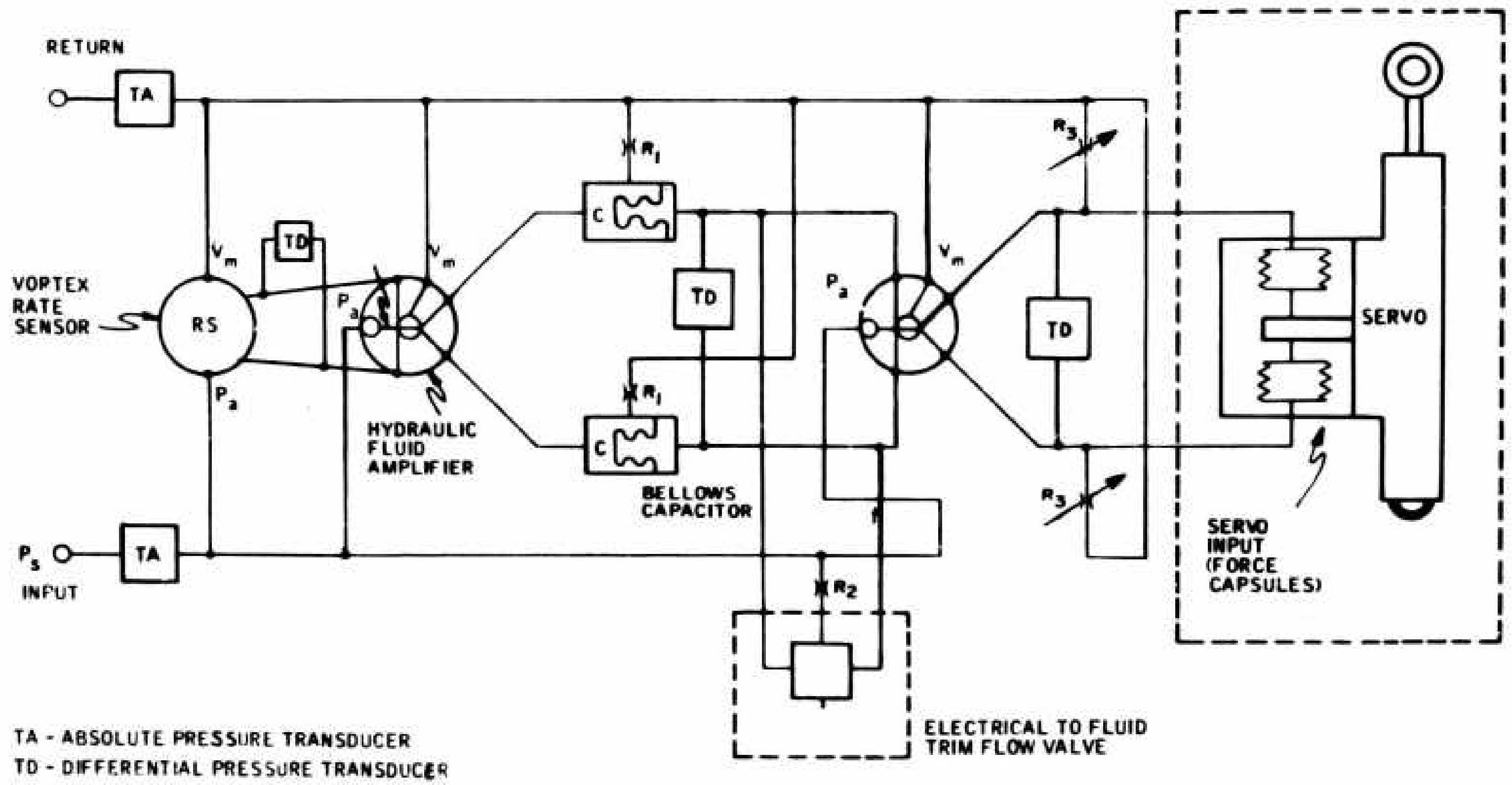

Figure 3. Flight System Circuit Diagram.

SECTION III

MECHANIZATION OR COMPONENT DESIGN

GENERAL

Figure 4 is a photograph of the complete fluidic yaw damper system shown schematically in Figure 3, with the exception of the servo. The rate sensor, amplifiers, and capacitors were designed to be mounted to a manifold plate. This allows the configuration of these components to be fixed, even if it becomes necessary to use a new circuit. This configuration resulted in considerable flexibility for changing both gain and time constant of the system, since the components and restrictors can be easily changed. Other features are the elimination of dead-ended cavities, which could trap air, and the elimination of external leakage.

RATE SENSOR

The rate sensor contained internal manifolding, eliminating the need for external plumbing. Nominal performance was:

Supply flow	=	2.5 gpm
Primary sink flow	≃	0.5 gpm
Secondary sink flow	≃	2.0 gpm
Scale factor	=	0.004 psi/deg/sec (loaded into an amplifier)
Noise	=	±1/8 deg/sec or less in control-frequency range
Time delay	=	<0.050 sec

Configuration of the secondary sink was designed to accommodate a viscosity-sensitive restrictor. Incorporation of this restrictor tends to decrease secondary sink flow when the fluid is cold, thereby increasing primary sink flow. Increased primary sink flow will increase the scale factor to compensate partially for viscous losses. At high temperatures, the inverse would occur. This compensates for the increased scale factor that normally occurs under these conditions and reduces the Reynolds number (and noise) in the primary sink. The viscosity-sensitive restrictor was not used during the flight test, but it was incorporated in post-flight checks.

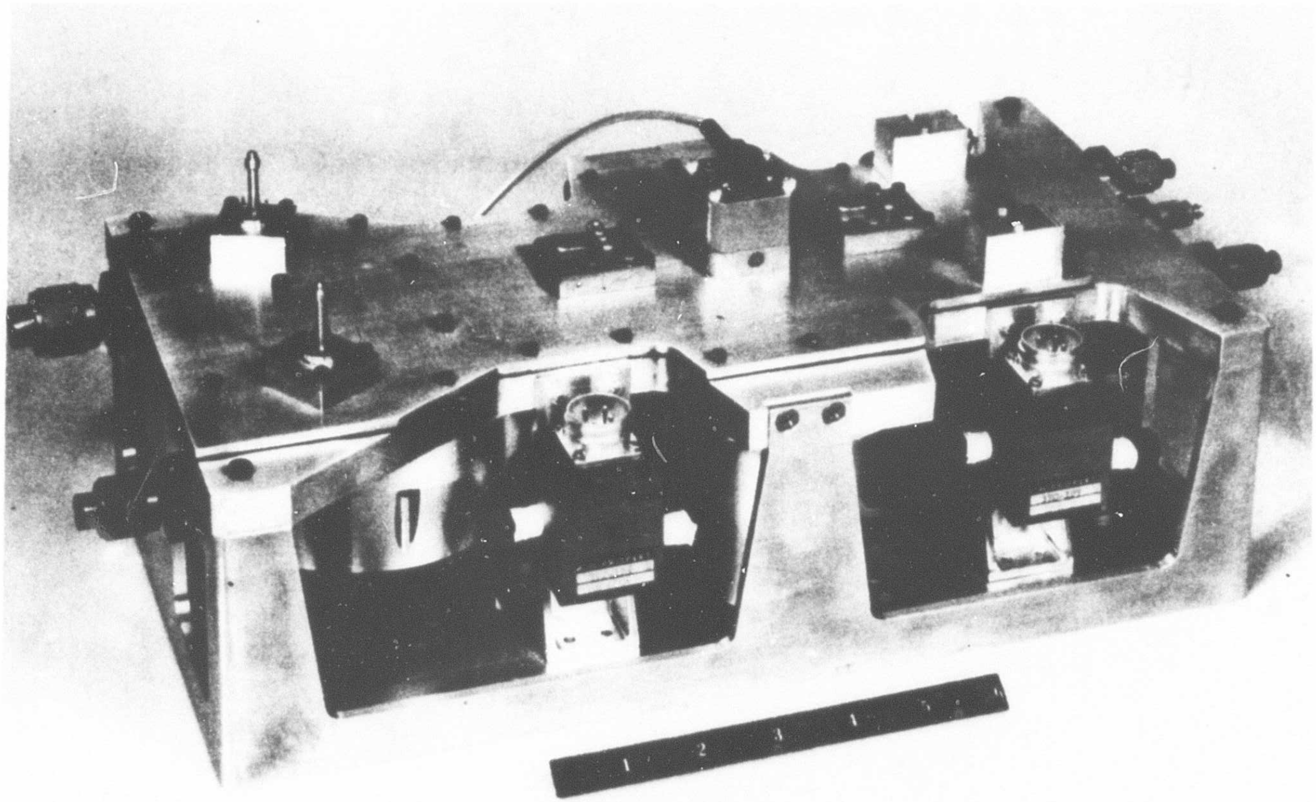

Figure 4. Fluidic Yaw Damper Flight Test Package.

AMPLIFIERS

Amplifiers used in this system were fabricated using a semiproduction technique: an electroforming process which eliminates both internal and external leakage. In this process a conductive wax mandrel (male amplifier) is injection molded to a nickel backup plate. This combination is then nickel plated and the wax is removed.

Samples of these amplifiers were proof pressure tested to 2000 psig to determine the quality of the bond between the amplifier and the base plate. Results indicate that the electroforming process will also be satisfactory for high-pressure fluidic applications where the supply pressure is 3000 psig or higher.

When these amplifiers were operating in the system, their nominal gain was 5.5. Typical dead-ended gain curves of these amplifiers are shown in Figures 5 and 6.

CAPACITORS

The bellows capacitors were purchased items; their size provided a nominal capacitance of 4×10^{-2} in.^{5}/lb.

RESTRICTORS

Amplifier output and input impedances provided the resistors for the R.C. network. A bias flow from the trim valve was used to increase the amplifier input impedance and to make it relatively independent of signal amplitude. The total resistance in the R.C. network was about 60Ω. This could be increased to 90Ω by using the maximum flow available from the trim valve. (A 0.010-inch orifice was placed in the inlet port of the trim valve to reduce the bias flow when operating at the 60-Ω conditions.) Small changes in time constant were accomplished with bias flow (resistance); large changes required a change in capacitance.

Other restrictors shown in Figure 2 were incorporated at high points to allow the removal of trapped air from various locations such as the capacitors and the dead-ended lines to the actuator. These restrictions are also capable of changing amplifier output impedance and system gain. In this system, gain was adjusted by changing system flow.

The sizes of the restrictors used in the final flight-test configurations were:

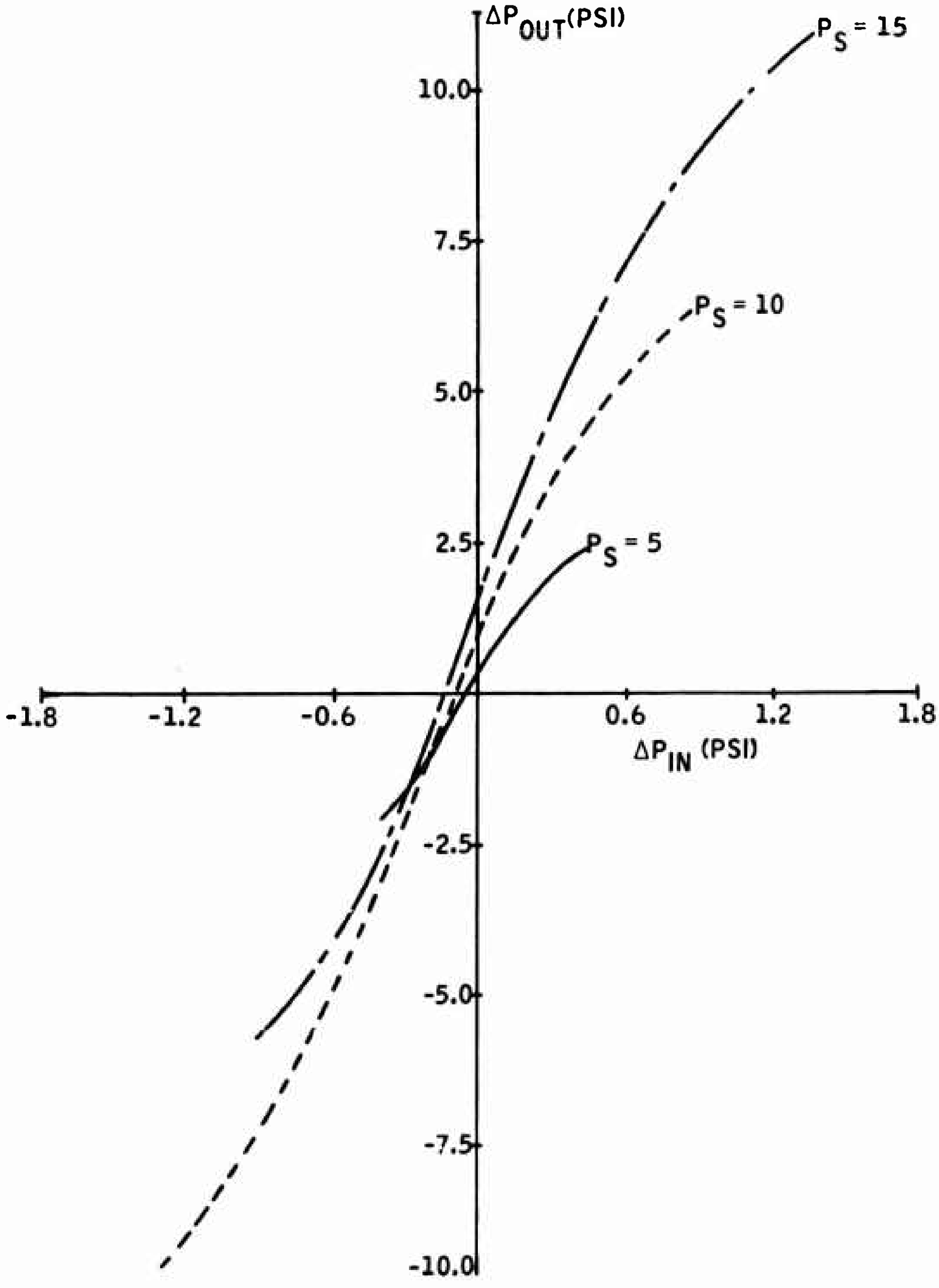

Figure 5. Preamplifier Gain Curve.

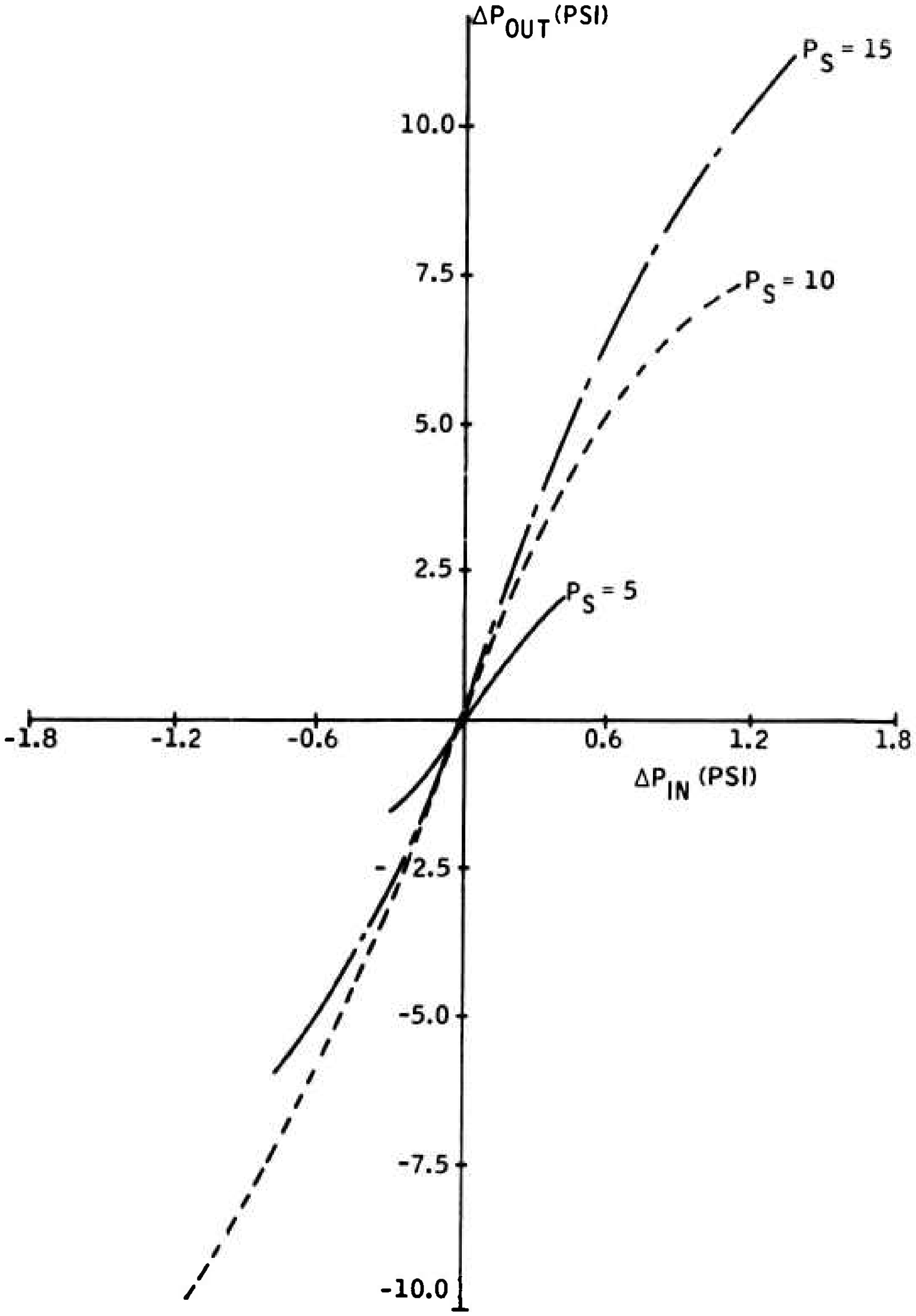

Figure 6. Power Amplifier Gain Curve.

R_1, capacitor bleed restrictor - 0.015 in. dia

R_2, trim valve flow limiter - 0.015 in. dia

R_3, output amplifier bleed restrictor - 0.010 in. dia

MANIFOLD PLATE

Configuration of the manifold plate is shown in Figure 7. Channels milled in this plate transmit supply, return, and signal flows to the various components. Since the instrumentation transducers are dead ended, it was necessary to make the connection with these transducers from the bottom of the plate. This prevented air from entering and accumulating in the transducers. Trapped air was a major concern due to its effect on system response.

TRANSDUCERS

The diaphragm in the pressure transducers acts in a manner similar to a bellows capacitor; this tends to reduce the response of the system. The transducer, measuring rate sensor output differential pressure, had a full-scale range of only ±1 psid and, therefore, had the most flexible diaphragm; capacitance of this transducer was 3×10^{-4} in. ^{5}/lb. It was determined that this transducer did have a noticeable effect on response, but a total system response was suitable.

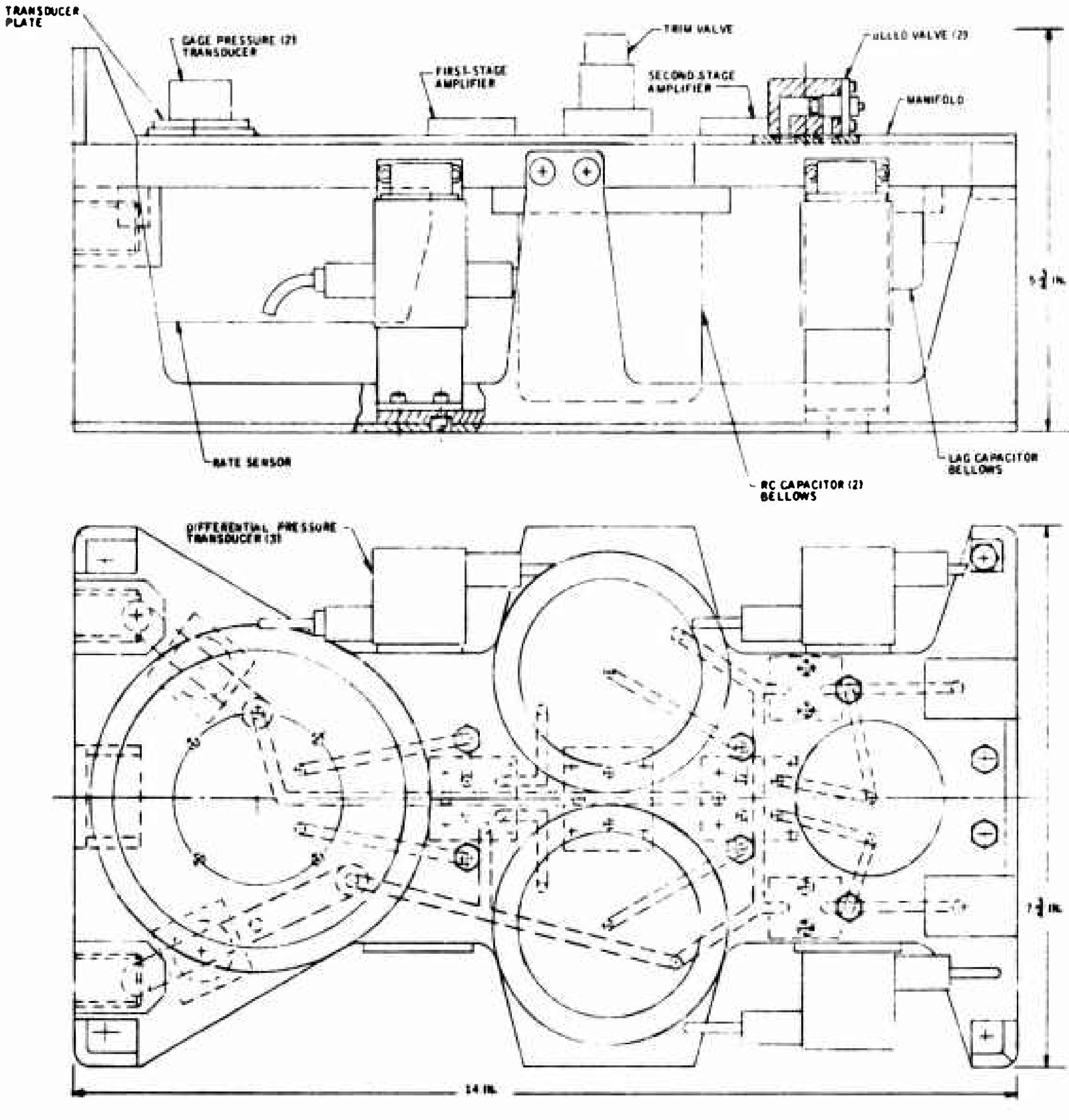

Figure 7. Manifold Plate.

SECTION IV

HYDRAULIC POWER SUPPLY

GENERAL

An "off-the-shelf" hydraulic power pack was used as part of the hydraulic power supply system. This pumping unit contains a reservoir, filters, internal relief valves, and a temperature-control valve. The entire power supply system is shown in Figure 8. (Note the heat exchanger on the right and the bypass valves on the left.) The power supply was considered as test equipment and is not typical of a prototype system.

HYDRAULIC POWER PACK

This power pack is a qualified unit designed to operate with Coolanol. Characteristics of this power pack are:

Maximum flow	=	3.75 gpm (MIL H5606)
Output pressure	$\leqq$	50 psi above return
Power	$\cong$	600 w of 115/220 v 400 cycles, 3-phase power
Reservoir capacity	=	45 in.^{3} (System normally filled to 25 in.^{3})
Dry weight	=	6.5 lb
Thermal control valve	-	Will maintain a system temperature of about 112°F when operating with a suitable heat exchanger

HEAT EXCHANGER

During the course of this program, it became expedient, because of delivery delays, to use a different heat exchanger from that originally planned: coil-ice instead of radiator-fan. The coil-ice heat exchanger, shown on the right side of Figure 8, holds enough ice to maintain the system's temperature for a period of about 1.5 hours.

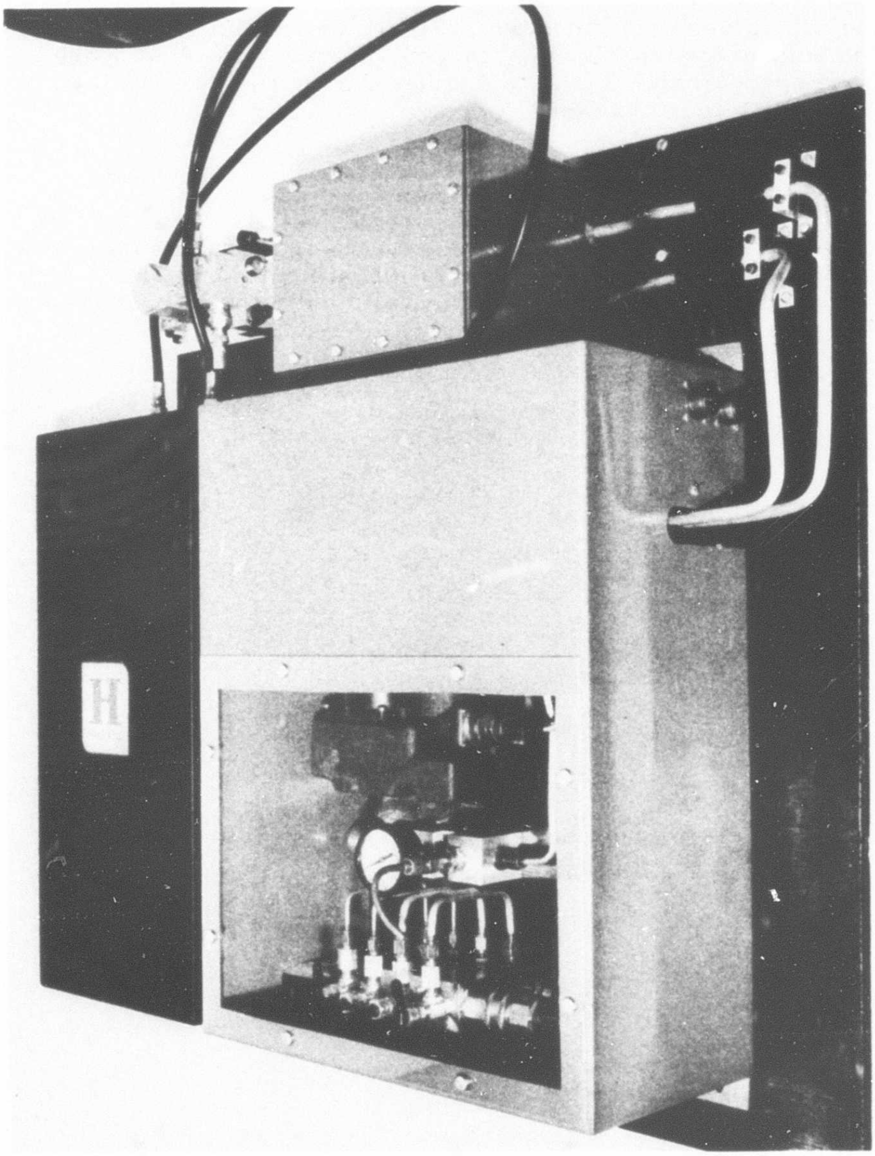

Figure 8. Hydraulic Power Supply.

VALVES - GAIN CHANGING

System gains can be changed by increasing or decreasing the flow to the system. The toggle valves (see left side of Figure 8) connect parallel flow paths which reduce system flow and, thereby, reduce gain when opened. Changes from one predetermined gain to another during flight testing were accomplished with these valves.

OIL-LEVEL INDICATOR

The pressure gage between the pump and the gain changing valves indicates the volume of fluid in the reservoir. The relationship between volume and pressure is shown in Figure 9. This curve is valid only when the ambient pressure is 14.7 psia.

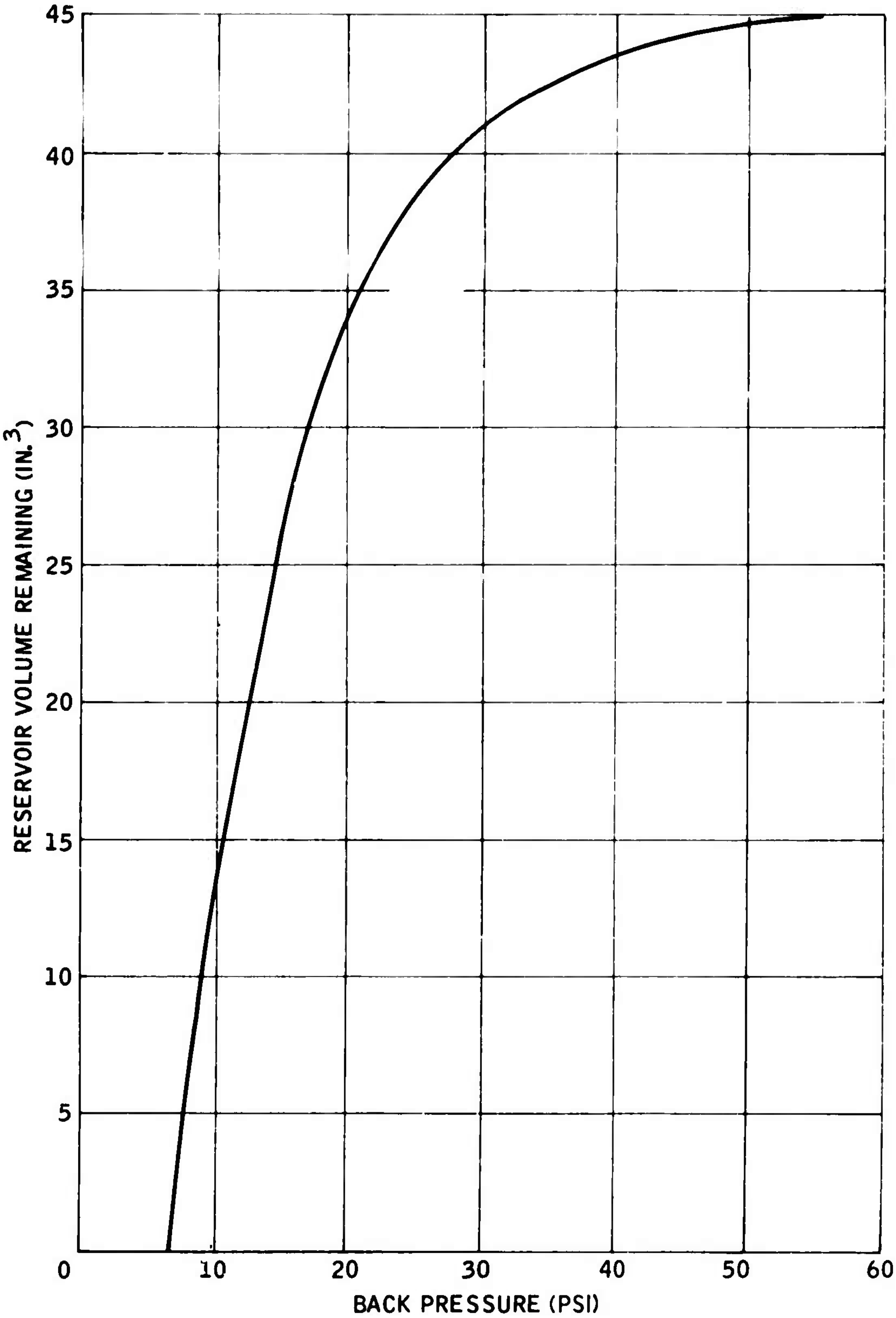

Figure 9. Reservoir Calibration.

SECTION V

SYSTEM TEST RESULTS

The system was designed to permit individual evaluation of the various components and circuits on the prototype manifold block. As an example, the rate sensor could be removed and replaced with a trim valve mounted on an adapter plate. All testing was accomplished with the specific components or circuits mounted on this manifold plate.

HIGH-PASS TIME CONSTANT

A hydraulic tilt table driven by a function generator was used to provide input signals into the system. Preliminary time constant data were obtained using step inputs and observing the time required for the output signal to decay to 63 percent of its peak value. Figure 10 is an example of the data obtained when a low-frequency, triangular wave input (square wave rate input) is used to control the tilt table.

Two methods were provided to allow adjustment of the high-pass time constant: capacitance can be reduced by using bellows with fewer corrugations, and amplifier input impedance can be reduced by decreasing the bias flow to the output amplifier (in this case, by placing a restrictor in the input to the trim valve). Bellows can be replaced when large changes in time constant are required, and trim-valve orifices can be changed when small adjustments are required. These techniques were used for the initial adjustment and were available, if needed, during the flight tests.

Other methods of modifying the high-pass time constant would be to change the amplifier size or to change the preamplifier output impedance through the use of different bleed restrictors on the output lags. These techniques were not evaluated in this program.

Final time constant determination was accomplished by evaluating the frequency response curves.

FREQUENCY RESPONSE

During development, frequency response curves were obtained at two input amplitudes: ±3 deg/sec and ±7 deg/sec. Oil temperature was 110°F, system flow was 2.54 gpm, and the system was connected to the actuator. The actuator was operating using a 1000-psi supply. Response curves shown in Figures 11 and 12 indicate the response of the complete system, including the actuator.

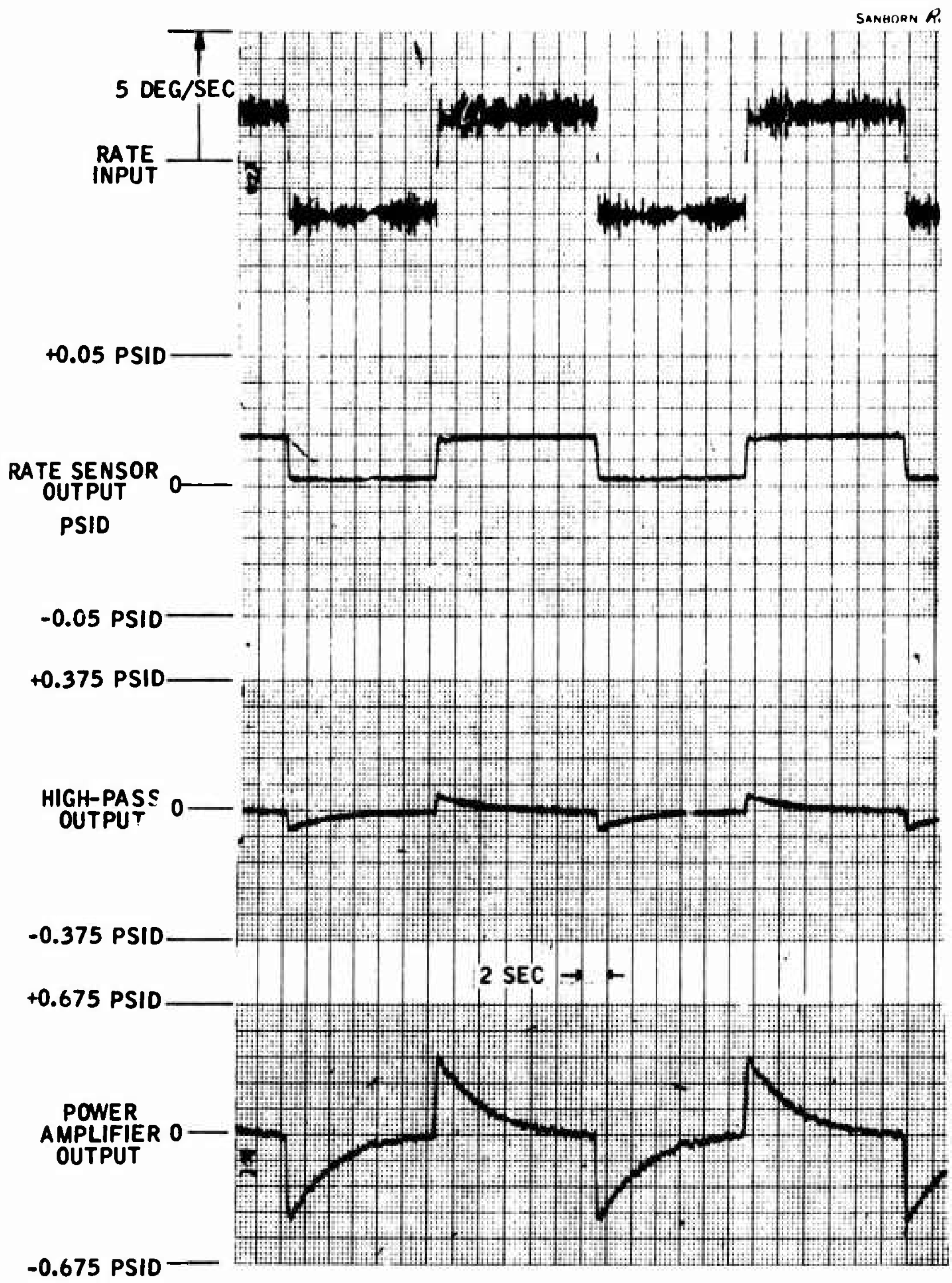

Figure 10. System Step Response.

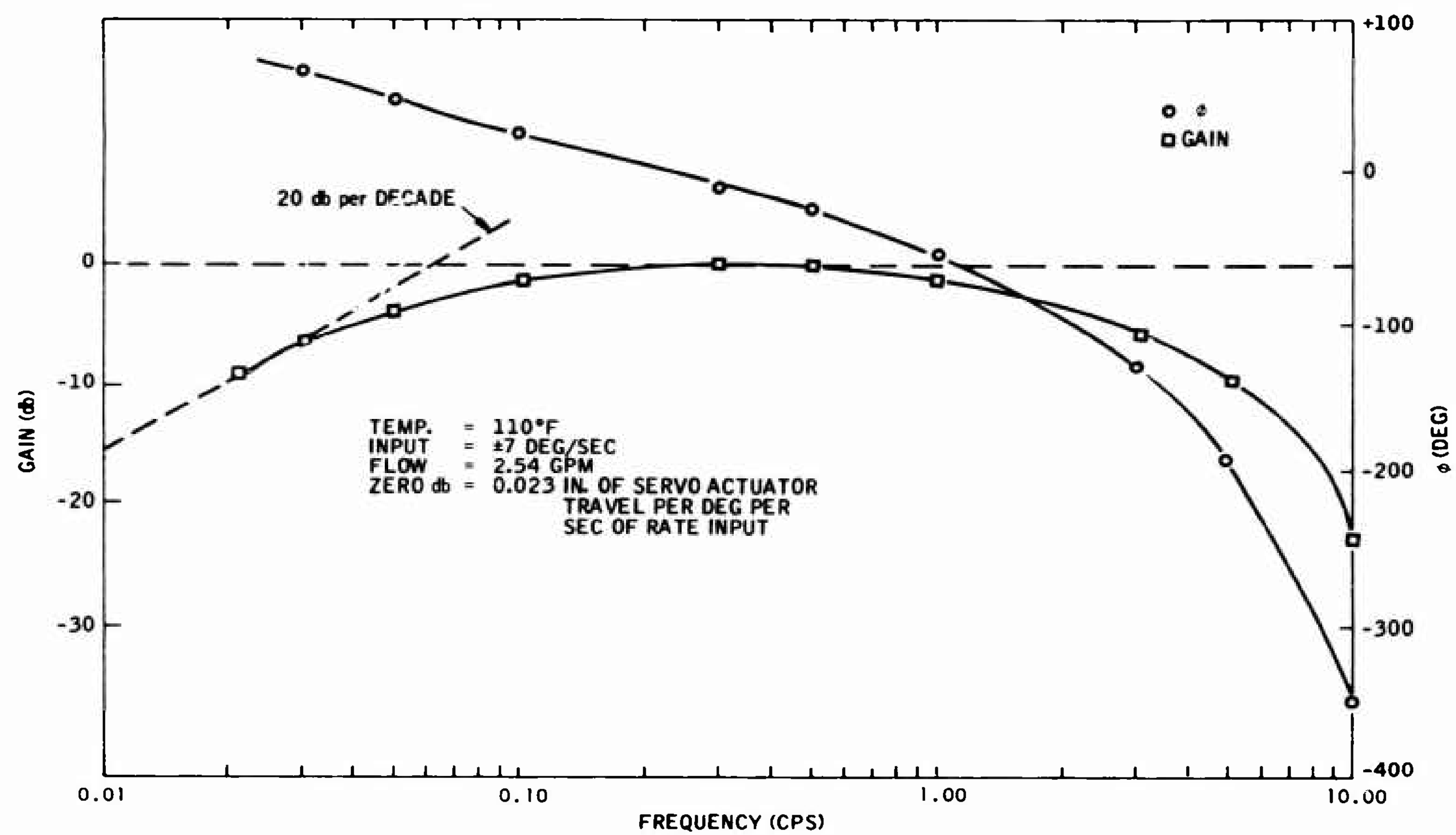

Figure 11. System Frequency Response (Large Amplitude).

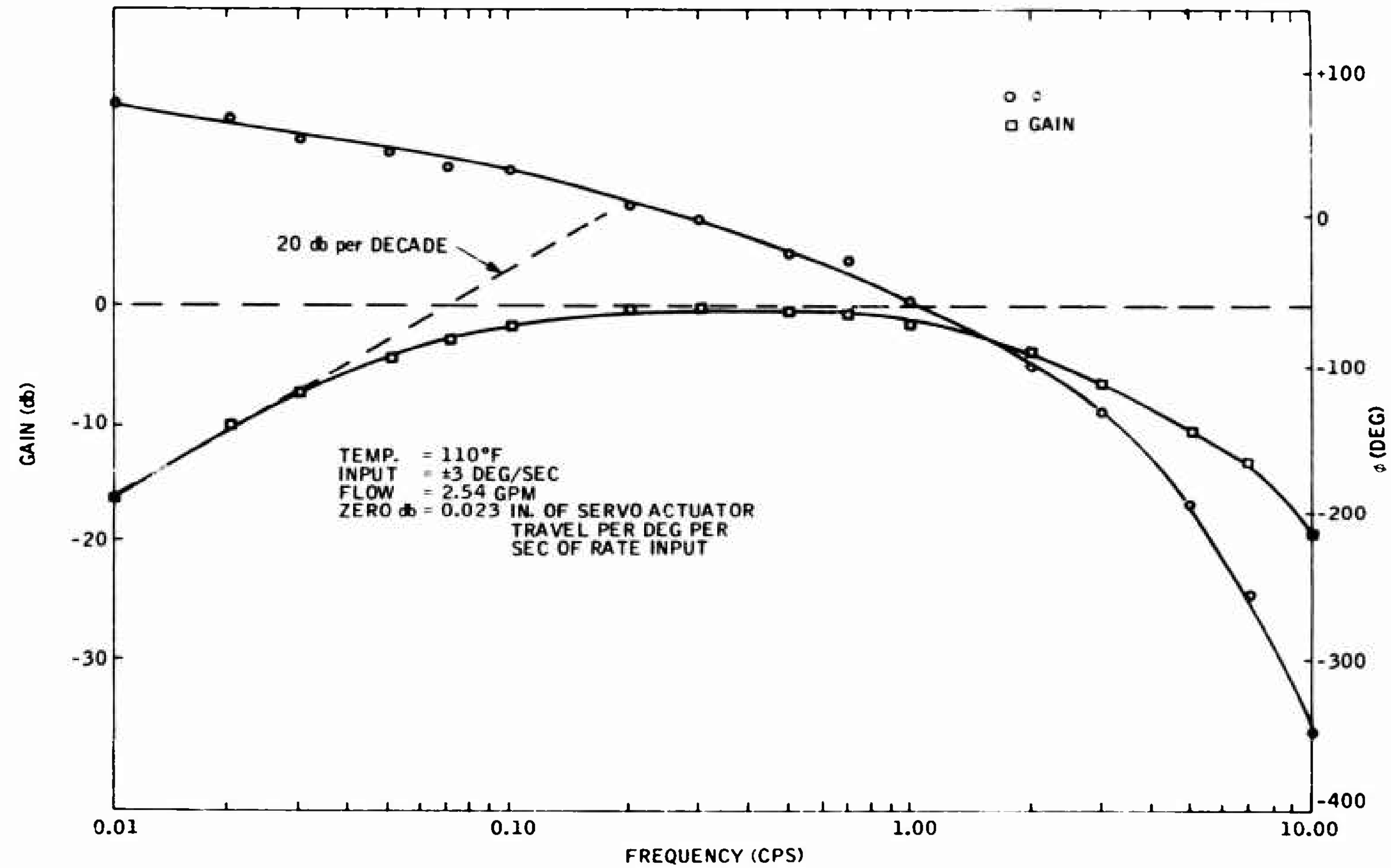

Figure 12. System Frequency Response (Small Amplitude).

These curves present an excellent example of a fluid system accurately duplicating the performance dictated by the design requirements. The curve taken at an amplitude of ±3 deg/sec provides several interesting observations. One is that the scatter in the data is extremely small. A 20-db/decade line drawn in Figure 11 shows how accurately the amplitude ratio curve duplicates the characteristics of

$$\frac{KS}{2.5S+1}$$

Note that the -3 db point occurs where this 20-db/decade line crosses zero db, as would be obtained with a perfect duplication of the above transfer function. Phase lead at 0.065 cps is slightly less than 40 deg, as expected. The difference between this and the ideal 45-deg phase lead is largely due to phase shift from sensor time delay and higher-frequency lags.

Figures 11 and 12 show that system response is relatively independent of input amplitude.

EFFECTS OF TEMPERATURE AND FLOW

Preliminary tests were performed on the system to determine the magnitude of temperature and flow regulation required. These data are shown in Figure 13.

Relative sensitivity to flow and temperature depends upon the operating conditions. For this reason, a great deal of care must be exercised when using the following generalities:

Percent gain change per percent of flow change = 1.7

Percent gain change per °F = from 0.7 to 1.0

Sensitivity to temperature is greater at the lower temperatures.

To maintain gain within ±20 percent of its design value, it would be necessary to control temperature to within ±20°F of the temperature regulator setting while maintaining flow within ±10 percent of flow regulator setting or better.

Selection of the hydraulic power supply described in Section IV eliminated the immediate problem of change in gain with flow and temperature. This system controlled the temperature to about 112 ± 2°F and the flow to better than ±1 percent of the required 2.54 gpm.

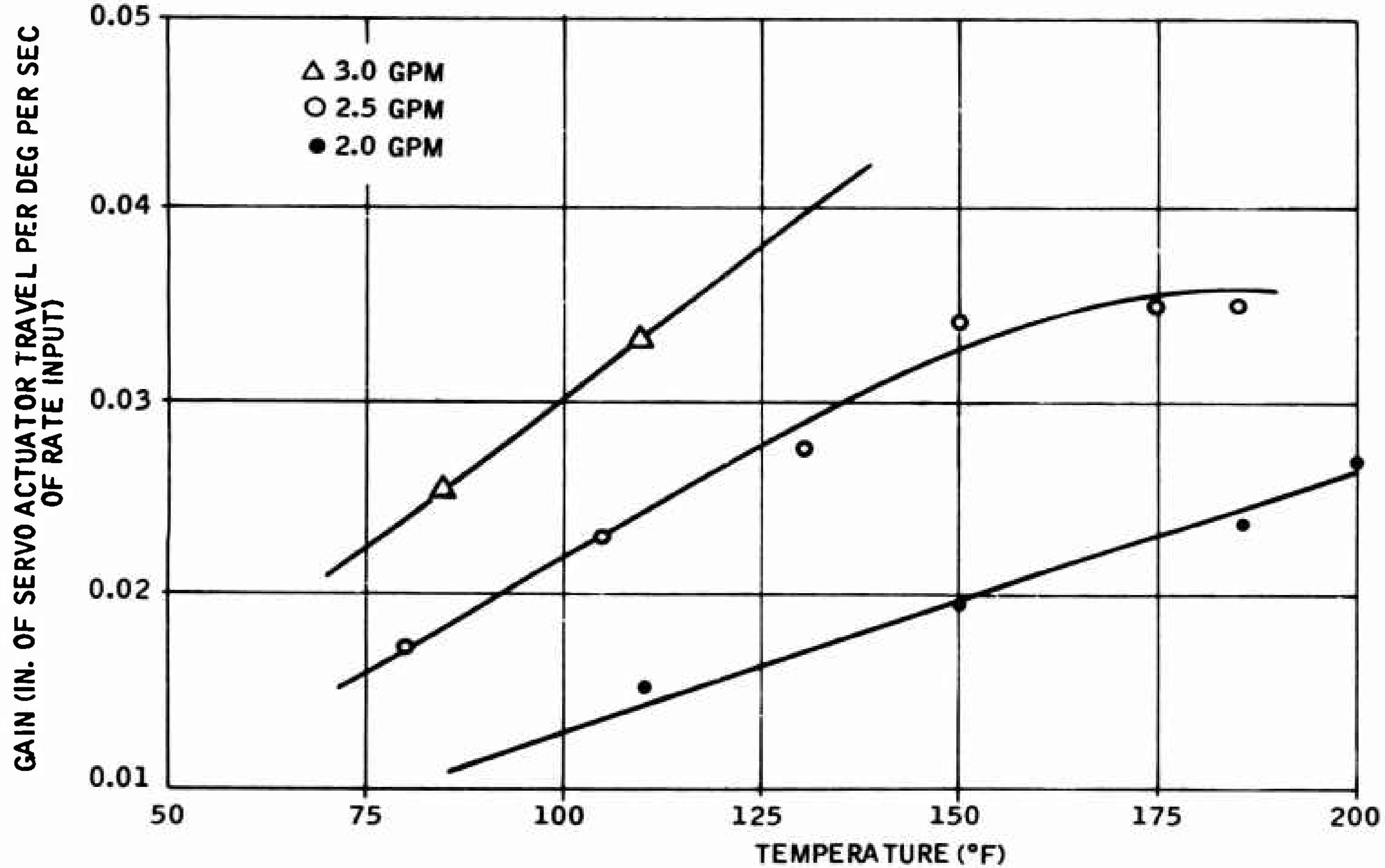

Figure 13. Preliminary Data on Gain as a Function of Temperature.

RATE SENSOR TEMPERATURE COMPENSATION

Design goals were to reduce the effects of oil viscosity on system performance, with special emphasis on the temperature range from +60°F to +185°F. Tests were performed on a test fixture which closely duplicated the internal geometry of the system rate sensor. A schematic of this geometry is shown in Figure 14. The primary and secondary sink flows are manifolded together internally in the flight-system rate sensor. The test fixture differs from the flight-test sensor in that it contains numerous pressure taps and includes provisions for measuring the flow split between the primary and secondary sinks.

The rate sensor pickoff is a restrictor which is sensitive to fluid viscosity (length = 0.5 in., area = 0.0079 in.^{2}, hyd dia = 0.061 in.). The secondary sink is more like a viscosity-insensitive orifice (length = 0.15 in., area = 0.026 in.^{2}, hyd dia = 0.182 in.). The pickoff and secondary sink are parallel flow paths to return, with approximately 20 percent of the flow passing through the pickoff sink at normal operating temperatures. When fluid viscosity increases, resistance of the primary (pickoff) sink increases, and flow through this path decreases. Figure 15 shows primary sink flow variations as a function of fluid temperature.

The adverse change in flow split between the sinks creates two problems: pickoff scale factor, which is proportional to flow, will decrease at cold temperatures; and Reynolds number and noise at the pickoff will increase at high temperatures.

A viscosity-sensitive restrictor (length = 0.6 in., area = 0.075 in.^{2}, hyd dia = 0.024 in.) was installed in the secondary sink flow path. Size of the secondary sink should be increased to compensate for the additional pressure drop of the restrictor at the nominal operating conditions. In this test, secondary sink size was not changed, but the sensor was tested at a lower flow condition (1.5 gpm) where the dead-ended scale factor was nearly the same as that of the original sensor. Note in Figure 15 that primary sink flow increases at the low-temperature condition. This sensor, with the viscosity-sensitive restrictor added, was also tested at the original flow of 2.5 gpm with the same desirable result of higher pickoff flow at low temperature.

The major reason for designing a sensor where the primary sink flow increases at cold temperature is to obtain a constant gain over a wide range of fluid temperatures. Figure 16 shows that this condition was approached at the 1.5-gpm condition and was obtained at the 2.5-gpm condition.

Other tests were performed after the post-flight checkout (Section VII). In these tests, the viscosity-sensitive restrictor was installed in the flight-test system.

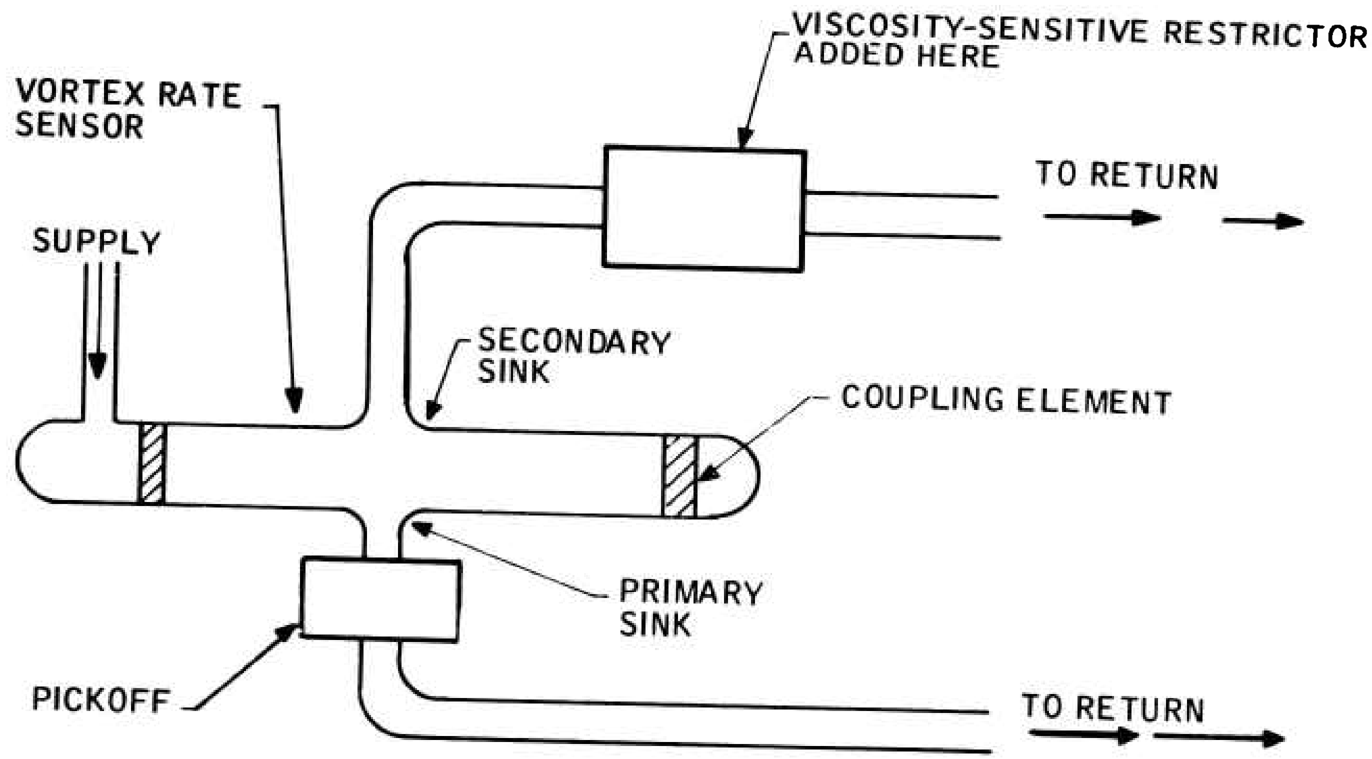

Figure 14. Rate Sensor Schematic.

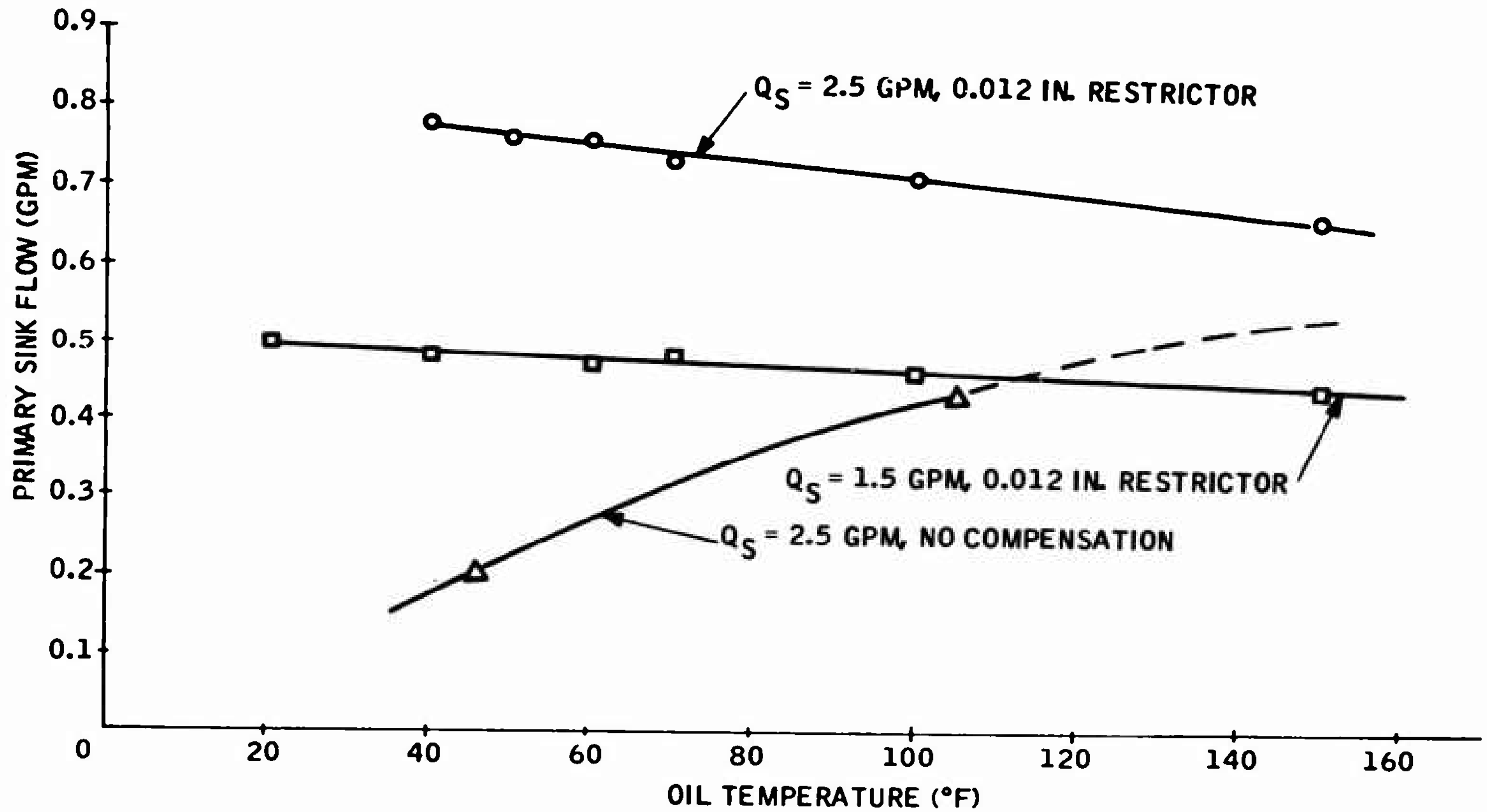

Figure 15. Primary Sink Flow Versus Temperature.

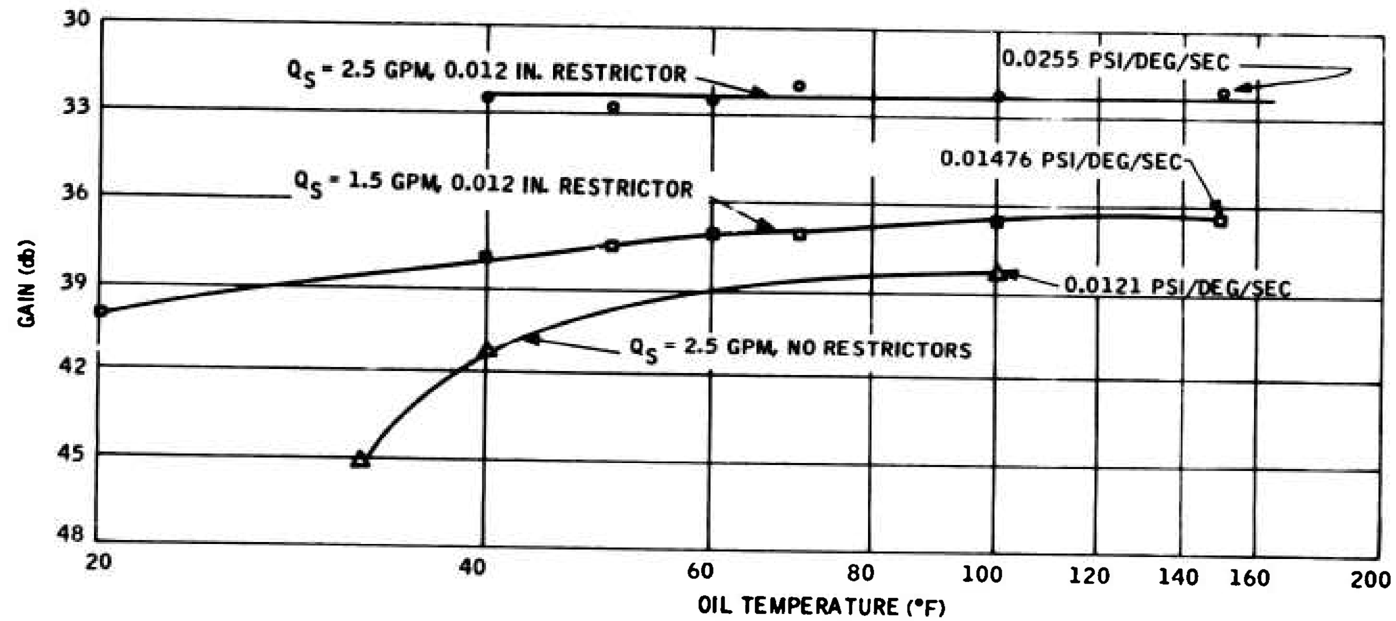

Figure 16. Sensor Gain Versus Temperature.

EFFECTS OF TRANSDUCERS ON SYSTEM PERFORMANCE

When testing began, the transducers created some problems, the most significant of which was noise. Air in the lines to the transducers would reduce both noise and response. Removal of air from one side of the transducer would result in a sharp increase in noise; removal of air from the other side would then cause a substantial reduction in noise. This noise problem did not recur later in the program, indicating that the design of the manifold plate was effective in preventing the accumulation of air in the region of the transducers.

The effect of transducers on system response can be seen in Table I.

TABLE I. EFFECTS OF TRANSDUCERS ON SYSTEM RESPONSE

Frequency	Rate Sensor Scale Factor (psi/deg/sec)	Rate Sensor Phase (deg)	Scale Factor at Bellows Output (psi/deg/sec)	Phase at Bellows Output (deg)
0. 5 cps with tdr	0. 00390	-9	0. 0160	-9. 0
0. 5 cps without tdr	--	--	0. 0187	-4. 5
5 cps with tdr	0. 00165	-121	0. 0123	-88. 0
5 cps without tdr	--	--	0. 0164	-72. 0

Bellows output amplitude and phase at 5 cps indicate that the transducer induces an attenuation of about 2 db and a phase shift of 16 deg. Effects of the transducer are substantially less at lower frequencies. Response of the transducer (as installed in the system) is poor. Resistance of the lines (0. 060 ID) from the system to the transducer contributes to its poor response. Larger lines would improve transducer response, but it would also allow the transducer capacitance (3 x 10^{-4} in.^{5}/lb) to have a greater effect on system performance. The other transducers had capacitances which were 0. 2 x 10^{-4} in.^{5}/lb or less, and their effects on system performance are negligible.

FILTER CAPACITOR

The system was designed so that a filter capacitor could be installed at the output of the last stage amplifier. This capacitor was removed from the system when it was determined that the system noise level was acceptable.

SECTION VI

ACCEPTANCE TESTS

The Appendix is an Engineering Test Report of the fluidic system acceptance tests. These tests include vibration, cold-temperature, frequency response, and closed-loop simulation with a computer.

The system was within specified performance limits for all conditions, except that gain at 10 cps was high by almost 4. 5 db. System response above 3 cps is relatively unimportant,provided peaking does not occur. Allowable system gain at 10 cps could probably be increased by more than 10 db without impairing system performance.

Satisfactory system performance was also demonstrated in a closed-loop, analog computer simulation. A diagram of the test setup is shown in Figure 17. The analog computer simulation is defined in Figure 18. System responses at 60, 90, and 120 knots are shown in Figures 19 through 21. Table II summarizes these results.

TABLE II. SIMULATED SYSTEM PERFORMANCE WITH AND WITHOUT FLUIDIC CONTROL

Flight Condition (knots)	Damping Ratio of Free Aircraft (Average of 4 points)	Damping Ratio with Fluid Control (Average of 4 points)
60	0. 29	0. 59
90	0. 34	0. 59
120	0. 35	0. 60

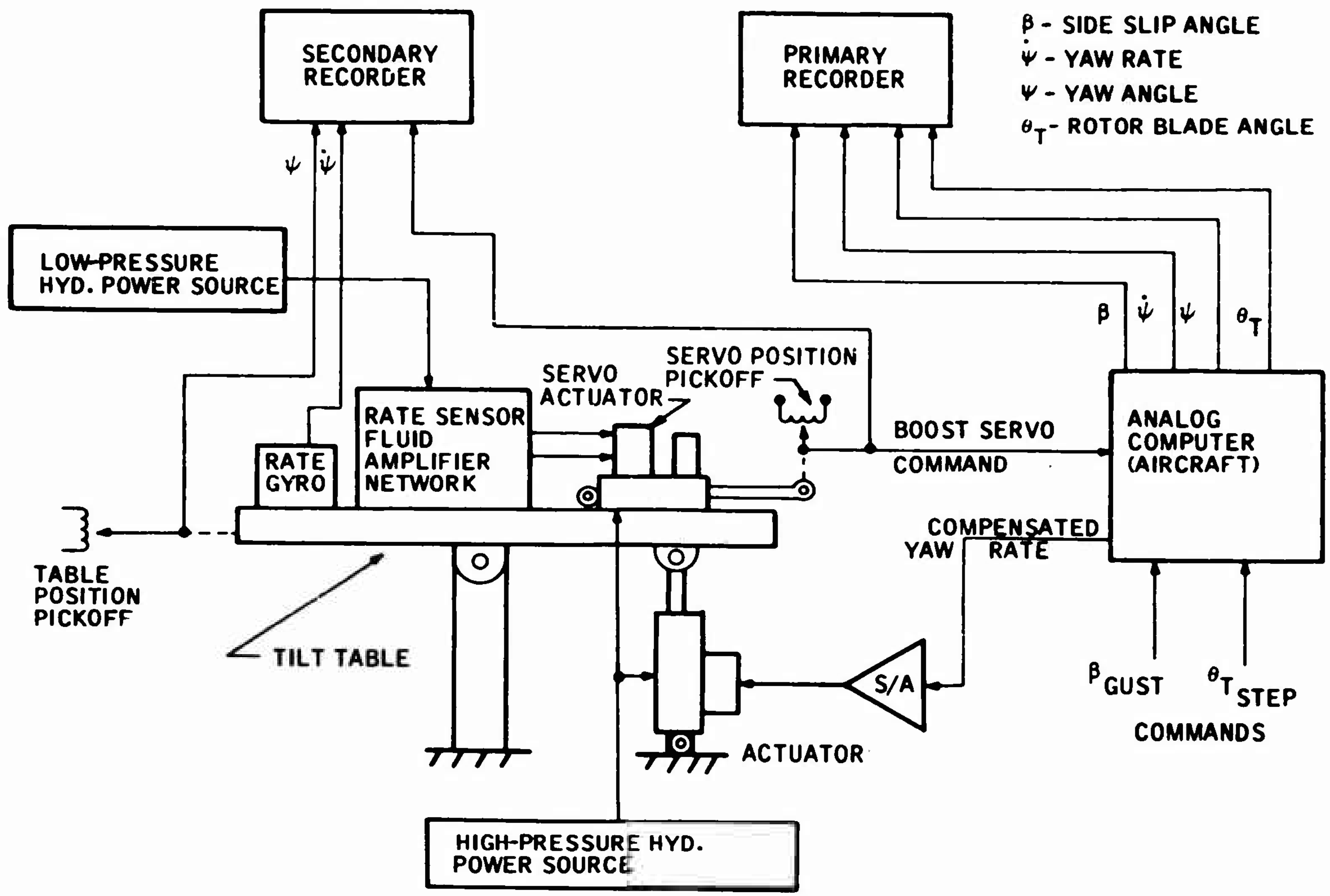

Figure 17. Acceptance Test Setup.

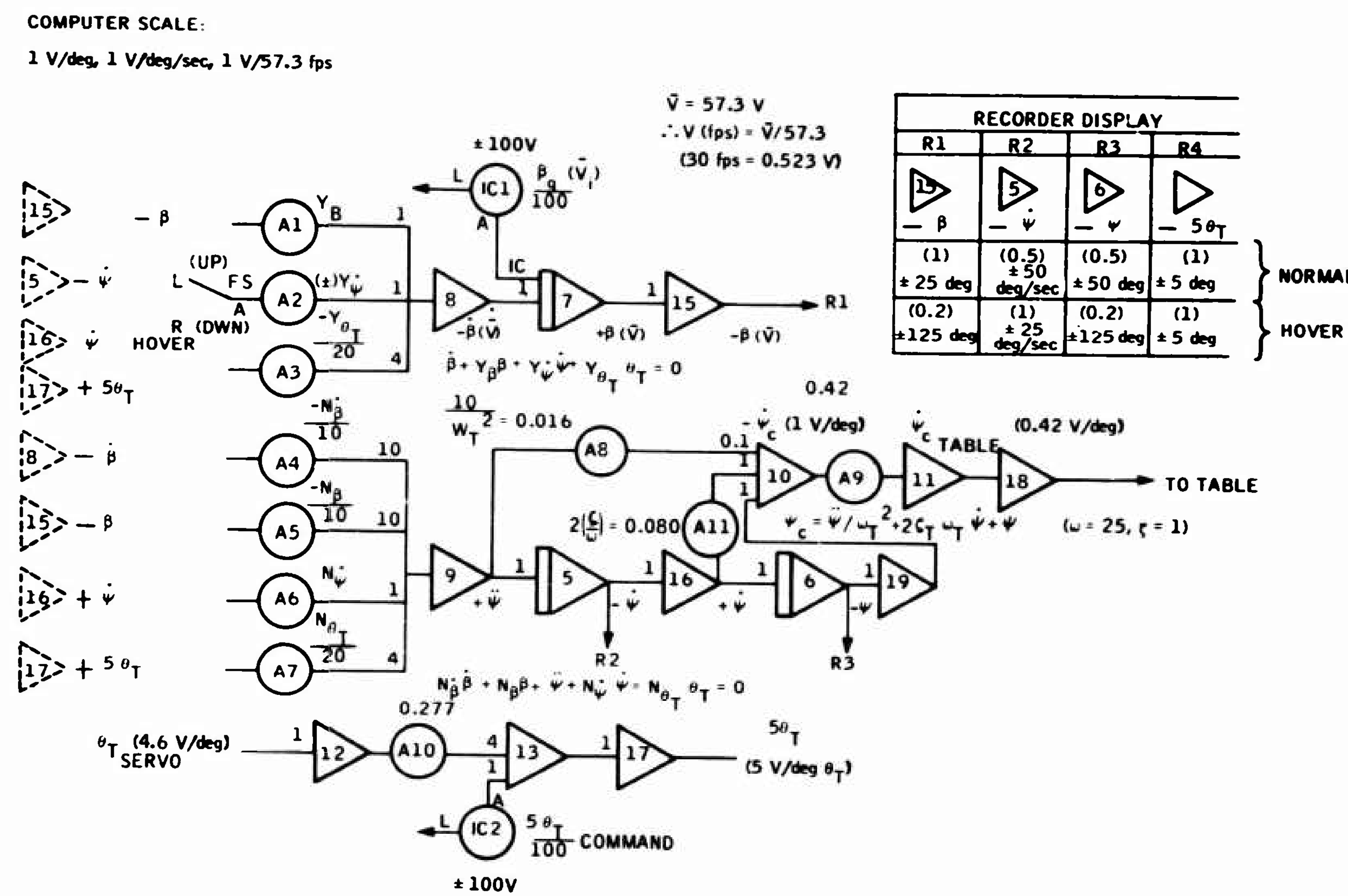

Figure 18. Computer Simulation.

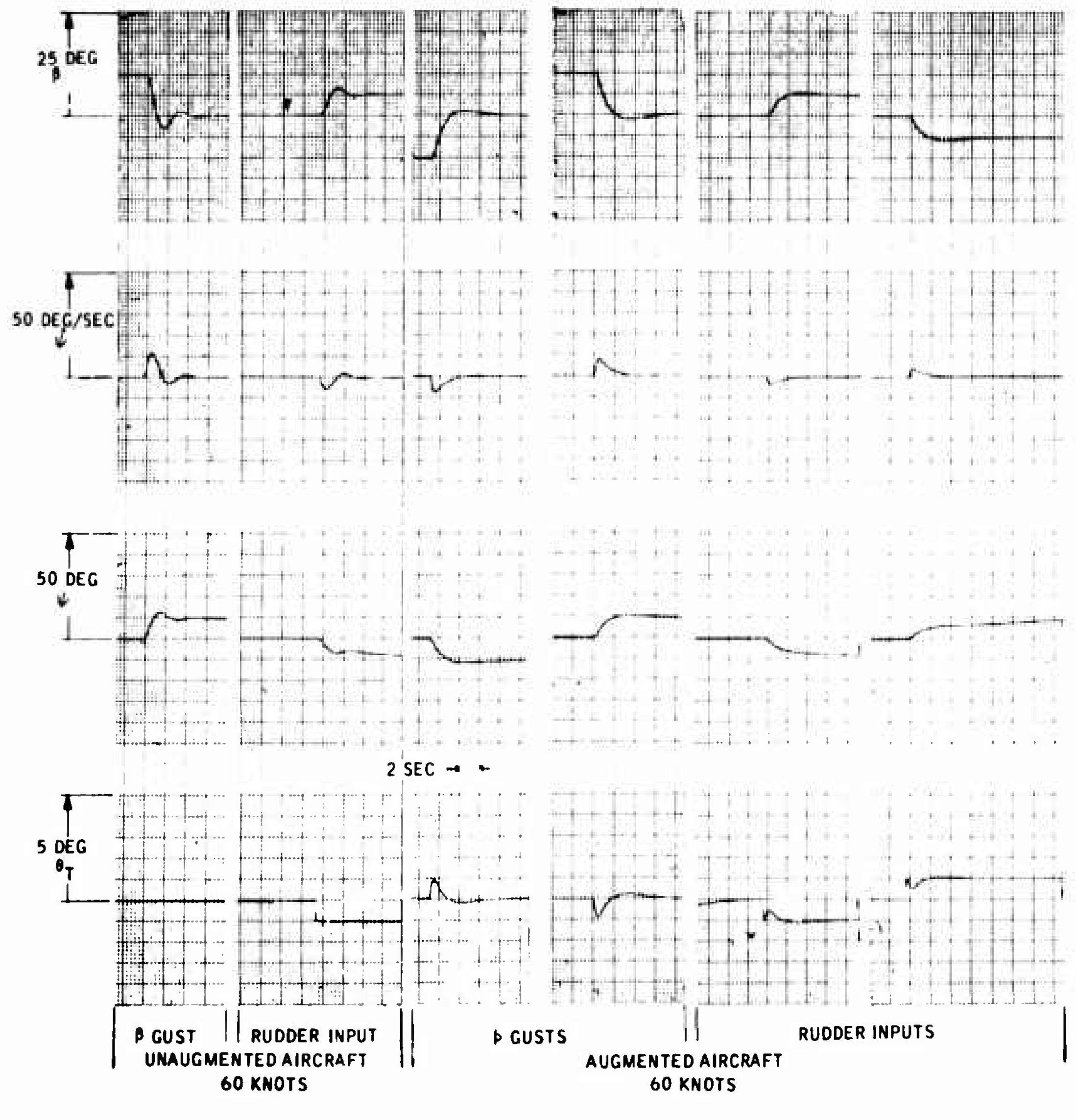

Figure 19. Closed-Loop Step Response at 60 Knots.

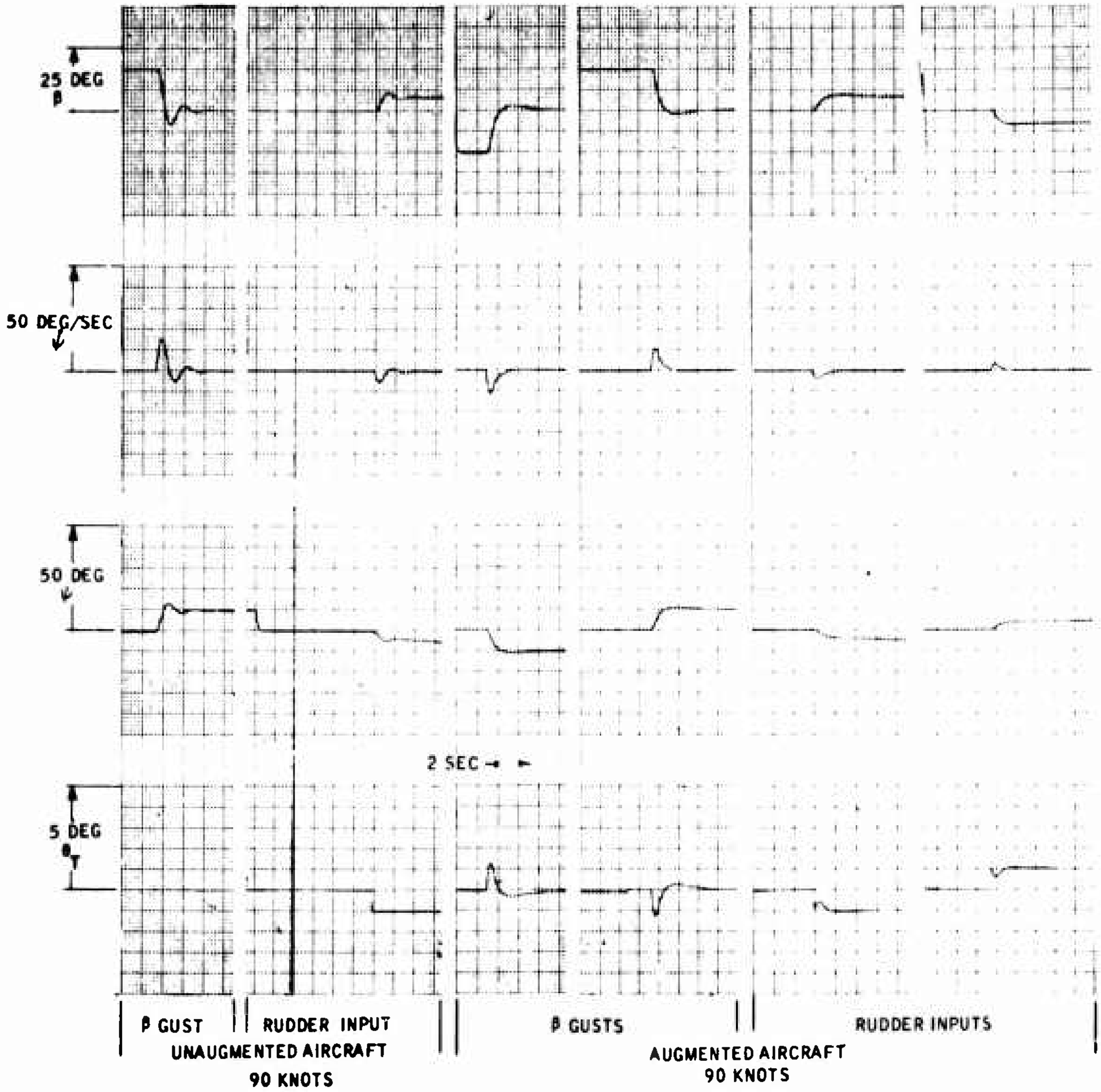

Figure 20. Closed-Loop Step Response at 90 Knots.

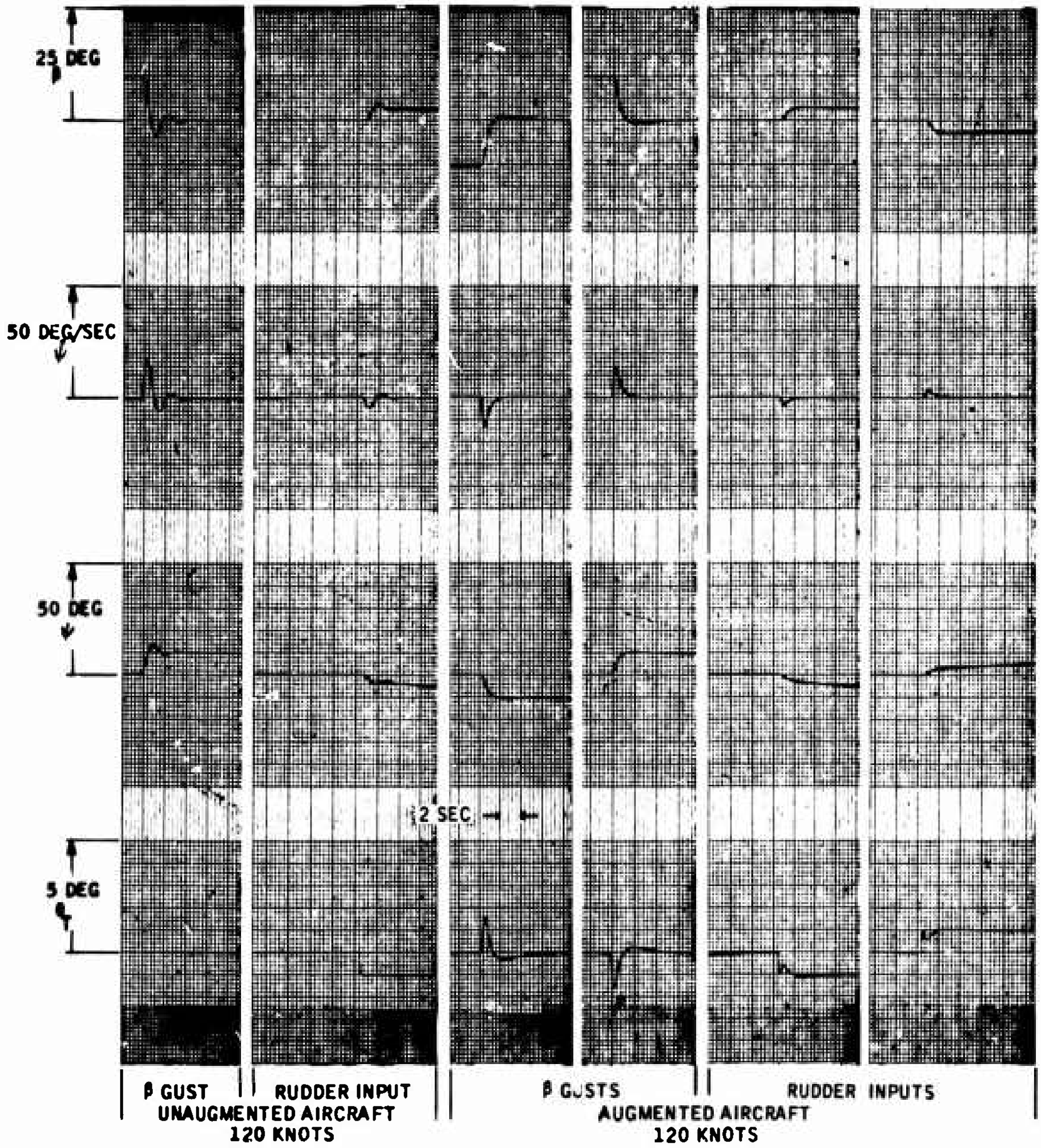

Figure 21. Closed-Loop Step Response at 120 Knots.

SECTION VII

POST-FLIGHT TESTS

OBJECTIVES

Post-flight tests were performed for the following reasons:

1. To determine system performance at the gain settings and actuator supply pressures used during the flight

2. To demonstrate that the gain change with temperature can be substantially reduced with a simple, rate sensor modification

HARD-OVER PROBLEMS

Post-flight tests showed that the system was hard-over. The problem was traced to the servo (Figure 22), where a captive pin between one of the force capsules and the armature had become displaced, probably during preparation for shipment. When the pin was inserted, the system returned to null.

The most probable cause of this problem is that the servo was subjected to a condition where control pressure Pc2 was substantially lower than the reference pressure, causing the pressure capsule to contract and [illegible]ing the pin to drop. When the actuator was removed from the aircraft with the system reservoir charged to about 15 psig, the reference pressure could have exceeded Pc2 by as much as 15 psig. This type of failure could not occur in normal operation, since the reference pressure is always lower than the control pressures. A servo with a greater tolerance for pressure surges may be needed when the fluidic system is integrated with the aircraft-hydraulic system.

FLIGHT-TEST CONDITIONS

During the flight test the servo was operated with a 1500 psia supply pressure,as compared with 1000 psi during the development tests.

The following gain settings were used during the flight-test program:

Setting I — 0.15 deg rotor/deg/sec. This "design point" gain setting improved damping ratio from 0.3 to 0.6. Note: Linkage gain between actuator and tail rotor is 6.25 deg tail rotor per inch actuator travel.

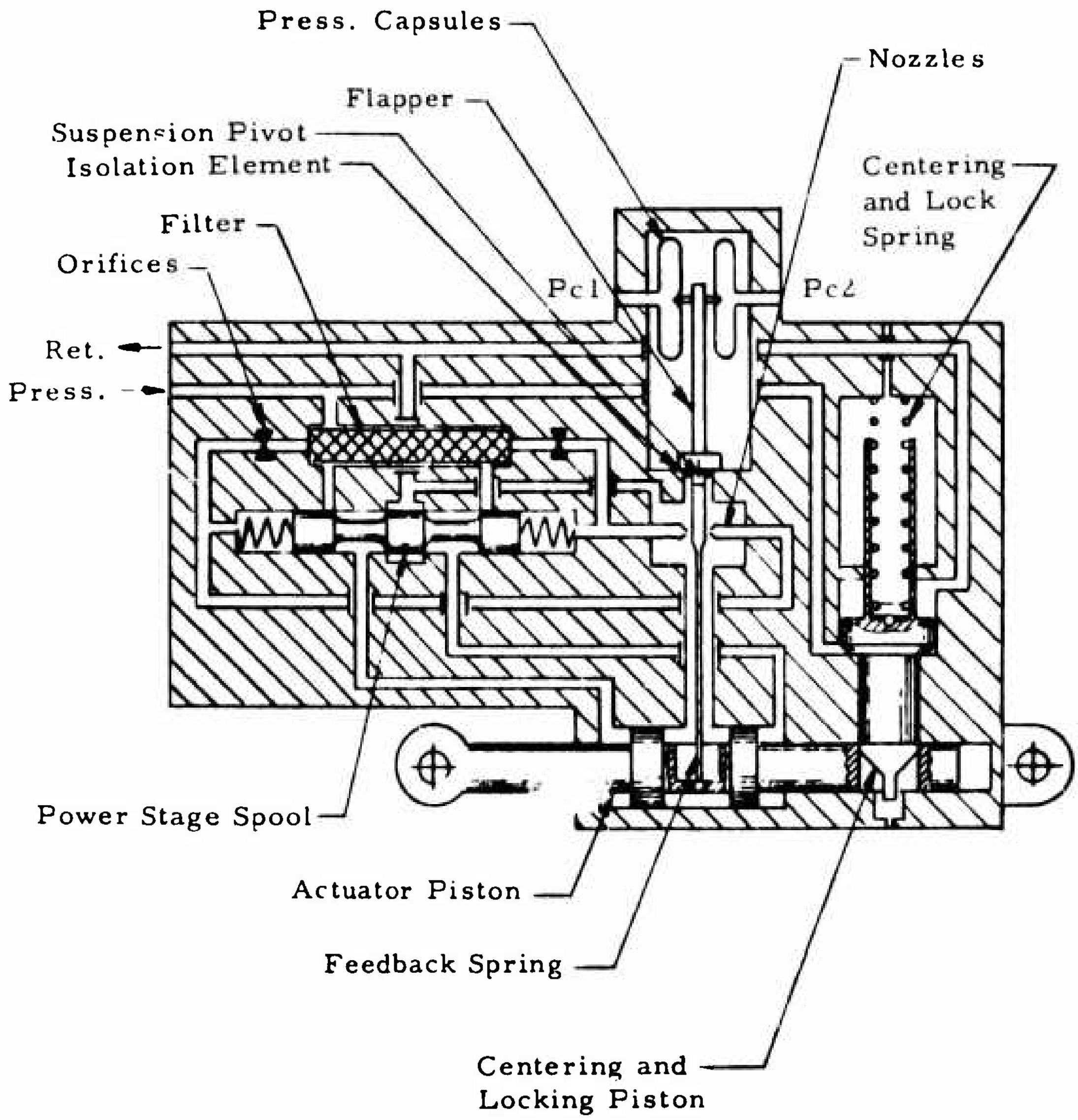

Figure 22. Servo Schematic.

Setting II - About 0. 30 deg rotor/deg/sec. This gain was definitely too high.

Setting III - About 0. 25 deg rotor/deg/sec. Most flight testing was performed at this gain, which was deemed to be a reasonable compromise between the hovering mode requirements and those at high-speed level flight.

SYSTEM TEST RESULTS

System gain and response at the various settings are shown in Figure 23. Gain at Setting I compares very closely with the results of the preflight acceptance tests shown in the Appendix. The curve shows the effect of using 1500 psi on the servo. The higher pressure results in higher response above 5cps, but it has an insignificant effect on gain. Response curves indicate that the characteristics at each gain setting are close to those assumed during the flight test. Phase of these curves is shown in Figure 24. Higher phase shift at the lower gains is due to the higher sensor time delay at the lower flows.

TEMPERATURE COMPENSATION TEST RESULTS

One method of maintaining a constant rate sensor scale factor over a wide range of temperatures was discussed in Section V. A viscosity-sensitive restrictor was incorporated into the rate sensor of the flight-test system. Use of the compensating restrictor increases primary sink flow, which increases sensor scale factor. System flow was then reduced from 2. 67 to 1. 52 gpm in order to keep system gain at the same value of about 0. 15 deg rotor/deg/sec. This compensated system was also operated at a flow of 2. 04 gpm, where the system gain was close to the 0. 26-deg rotor/deg/sec condition used throughout most of the flight-test program.

Figure 25 shows sensor scale factor as a function of temperature for the above three conditions. The uncompensated sensor scale factor was reduced to 27 percent of its 100°F value when the oil temperature was lowered to 20°F. The compensated sensor retained 58 percent of its scale factor at the low-flow condition and 72 percent of its scale factor at the high-flow condition. Increasing the length or decreasing the hydraulic diameter of the compensating restrictor would greatly improve the low-temperature characteristics of this system.

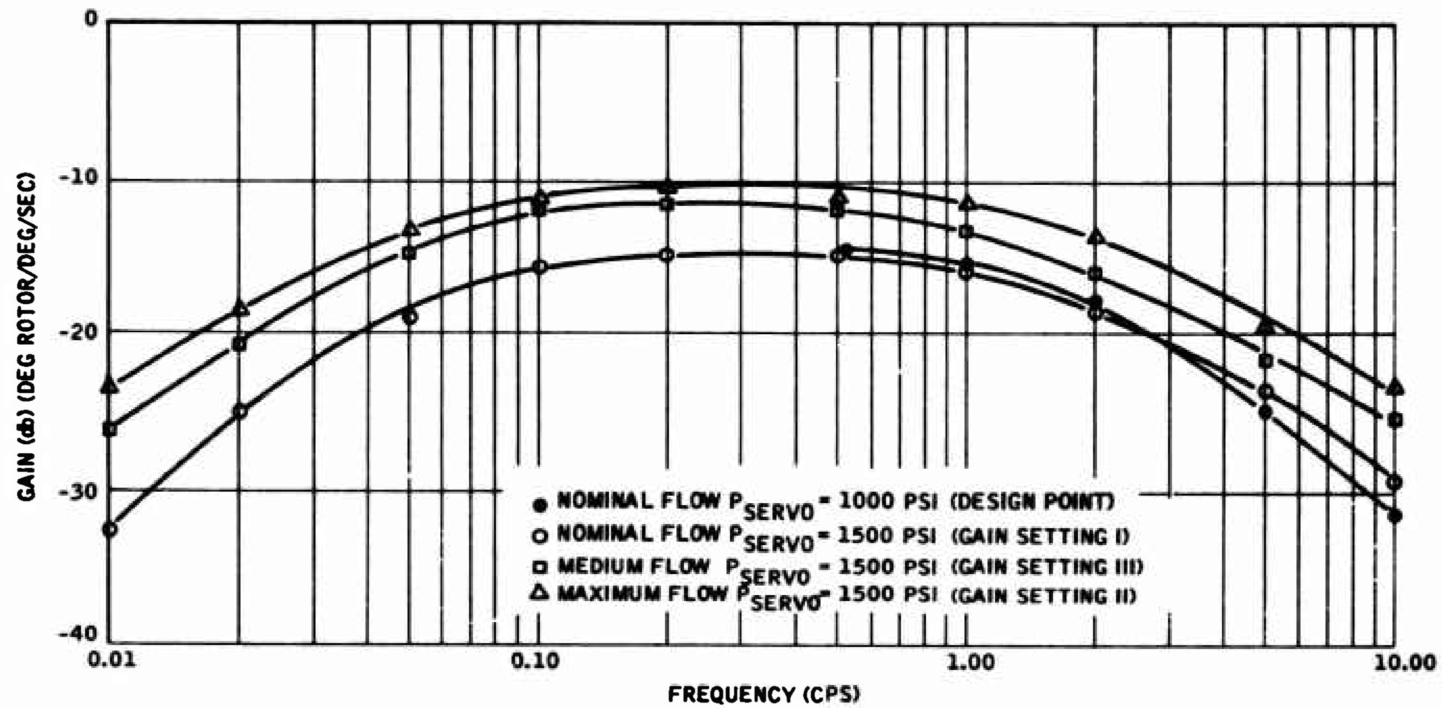

Figure 23. Post-Flight Test Amplitude Response.

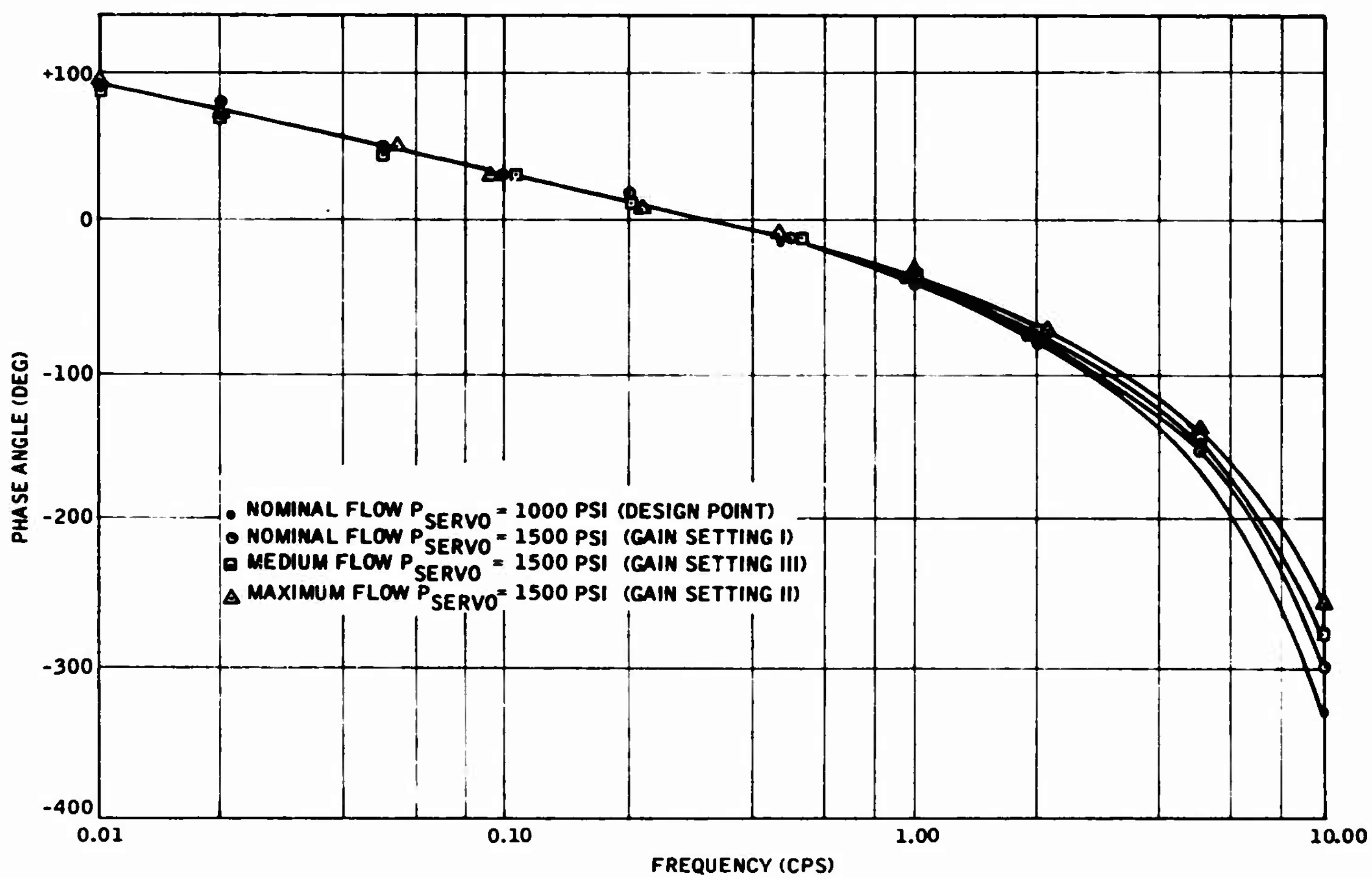

Figure 24. Post-Flight Test Phase Response.

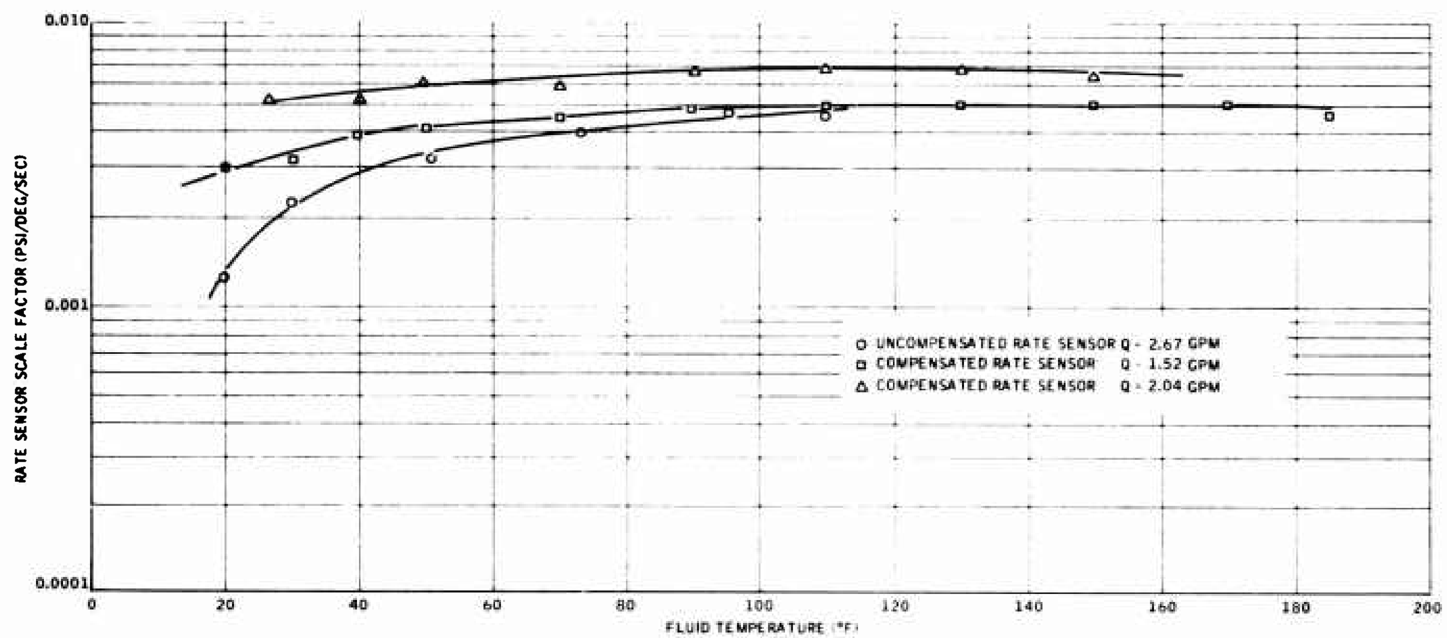

Figure 25. Effect of Compensation on Flight Test Rate Sensor.

Figure 26 shows the overall system gain as a function of oil temperature. Increased compensation should result in substantial improvement, since it would also improve the adverse flow split characteristics between the rate sensor and the amplifiers during low-temperature conditions.

Rate sensor data from Figure 25 can be compared with overall system performance to determine amplifier performance. With the uncompensated system, the overall gain at 40°F was 22 percent of that at 110°F. Since the rate sensor scale factor was about 60 percent of its 110°F value, the amplifier cascade has a gain of 0.36 times its original gain. Since two stages are used, each stage has a gain of 0.6 times its high-temperature gain.

The above procedure was used with the compensated systems operating at 2.04 gpm. In this case, the rate sensor and each amplifier had an attenuation to 0.8 at 40°F. The compensation improved each amplifier stage by an amount equal to the rate sensor improvement. This improvement in the amplifiers is due to the increased pressure across them at low temperature caused by the higher drop across the rate sensor (amplifiers and sensors are in parallel).

It is a coincidence that the gain of each component was attenuated by an equal amount at the 40°F condition and that the sensor compensation improved each component an equal amount. However, the example does show that the rate sensor compensation also improves the adverse flow split characteristics between the sensor and the amplifiers.

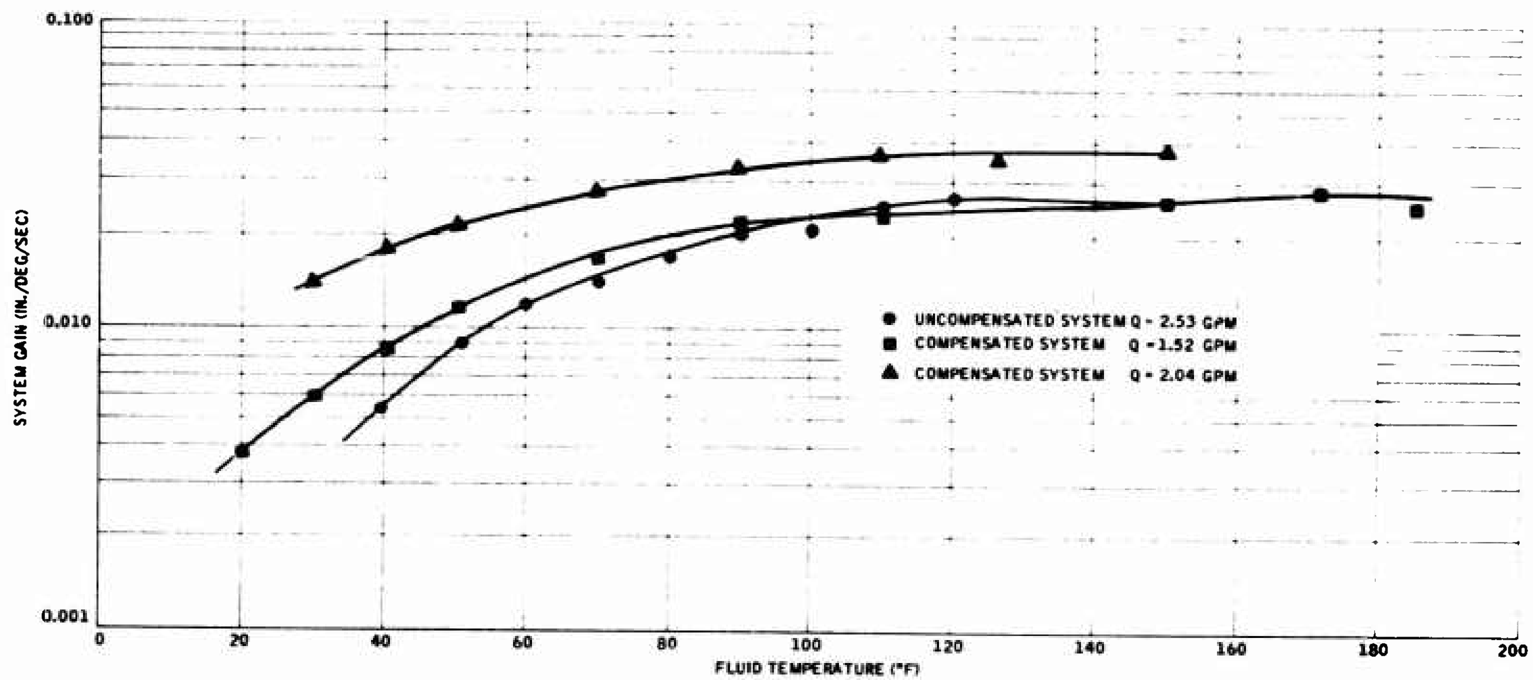

Figure 26. Effect of Compensation on Flight Test System.

SECTION VIII

CONCLUSIONS

As a result of the development program, the following conclusions are made:

- System performance was consistent and predictable throughout the program.
- Techniques used to minimize system noise were effective. Maximum noise with vibration levels of 0.8g or less was ±0.2 deg/sec. This performance is significantly better than what was anticipated at the start of the program.
- The series high-pass circuit greatly simplifies the mechanization of this system.
- The design approach used to compensate for changes in fluid viscosity appears to be practical for a wide range of temperatures. Compensation below temperatures of 0°F will be difficult with MIL-H-5606 oil.
- Self-bleeding techniques used on the control package should be extended to the servo.
- The servo should be designed to be more tolerant of excessive signal pressure surges. The design of the overall system and the operating procedures should be directed to minimizing these surges.
- All the design objectives of this program (described in Section II) were met or exceeded.

SECTION IX

RECOMMENDATIONS

It is recommended that further development be initiated in the following areas:

- Integrate the fluidic stability augmentation system (SAS) into the aircraft hydraulic system.
- Establish temperature-compensation techniques which maintain both the required gain and the time constant over a wide temperature range.
- Demonstrate the feasibility of a more complex control such as a three-axis SAS.
- Reduce both the size and the flow requirements.

APPENDIX

PREFLIGHT ACCEPTANCE TEST REPORT

ABSTRACT

Acceptance tests were performed on Hydraulic Fluidic Yaw Damper YG1023A to determine conformance to DS 12489-01, Part II. The Fluidic Yaw Damper YG1023A successfully passed the acceptance tests as described in DS 12489-01, Part II, with two exceptions. An Engineering Variation Authorization No. 68-1032 was written to waive these two parameter variations.

UNIT TESTED

One Hydraulic Fluidic Yaw Damper YG1023A built by the Technical Laboratory, Honeywell Aerospace Division, Minneapolis, Minnesota, was tested. This unit was built for the U.S. Army Aviation Materiel Laboratories, Fort Eustis, Virgina, under Contract DAAJ02-67-C-0056.

REFERENCE DOCUMENTS

Honeywell Detail Specification - DS 12489-01

PROCEDURE AND RESULTS

System Operating Conditions

For the acceptance tests, shunt valves 1 and 4 were opened, which allowed 2.69 gpm through the system. System operating temperature was 104°F, as measured on the outside of the rate-sensor cover.

Performance Test and Failure Criteria

System performance was determined several times during the acceptance tests. The performance test consisted of determining amplitude ratio and phase lag at 0.02, 0.50, 3.0, and 10.0 cps and determining system range ahead of the high-pass network. These data were then compared with Figure I of DS 12489-01 to determine if the system was operating properly. Table III lists the failure criteria as determined from Figure I of DS 12489-01.

TABLE III. FAILURE CRITERIA		
Frequency (cps)	**Gain (db)**	**Phase (deg) (cannot exceed)**
0.02	-27.00 ± 5.0	+47
0.50	-16.54 ± 5.0	-41
3.00	-18.86 ± 5.0	-162
10.00	-32.56 ± 5.0	-418

Range ahead of the high-pass network must be at least ±20 deg/sec.

Initial Previbration Test

While operating at room temperature, the system was subjected to the initial performance test. Table IV lists the performance test data.

TABLE IV. INITIAL PERFORMANCE TEST			
Frequency (cps)	**Gain (in./deg/sec)**	**20 log 6.62 Gain (db)**	**Phase (deg)**
0.02	0.0071	-26.56	+86
0.50	0.0250	-15.66	-15
3.00	0.0125	-21.66	-96
10.00	0.0105	*-23.16	-389

*Gain exceeds failure limit. Range was ± 20 deg/sec.

Vibration

The vibration test was performed according to MIL-STD-810A, Helicopter Curve A, Figure 514.2 and Time Schedule II of Table 514-II. Each of the three mutually perpendicular axes was vibrated in the following manner:

1. 0.8-g scan from 5 to 500 cps for 7.5 min
2. 2-g scan from 5 to 500 cps, four times, for 7.5 min at each cycle

From the 2-g scans, the major resonant frequencies were chosen; the system vibrated for 10 min at each resonant frequency. A maximum of four resonant frequencies was chosen. Four accelerometers were mounted on the system to monitor various structural elements. From the accelerometers and the system actuator position, the major resonant frequencies were determined.

The only system parameter monitored was the actuator position. Failure limits specified that due to system generated noise, the actuator movement could not exceed 0.030 in. peak-to-peak during 0.2-g vibration. The higher-level vibration (0.8 g) was conducted because the vibration machine could not control at less than the 0.8-g level. The system had to structurally pass the 2-g vibration scans and the resonant vibration.

Table V lists the system's maximum noise, its frequency during 0.8-g and 2.0-g scans, and the major resonant frequencies associated with each axis.

TABLE V. VIBRATION PERFORMANCE

Axis	Vibration Level (g)	Maximum Noise (in.)	Frequency (cps)
Vertical	0.8	0.010	10-20
	2.0	0.014	20
	resonant frequencies were 100 and 245 cps		
Longitudinal	0.8	0.010	7-20
	2.0	0.026	5-20
	resonant frequencies were 18, 80, 185, and 325 cps		
Lateral	0.8	0.006	9-50
	2.0	0.026	20
Resonant frequencies were 50, 230, 320, and 500 cps.			

The system successfully passed both noise and structural criteria during the vibration tests. Total vibration time was 212.5 minutes.

Post-Vibration Test

Table VI lists the system performance during the ambient-temperature test after vibration.

TABLE VI. POST-VIBRATION PERFORMANCE TEST

Frequency (cps)	Gain (in./deg/sec)	20 Log 6.62 Gain (db)	Phase (deg)
0.02	0.0071	-26.56	+80
0.50	0.0237	-16.08	-11
3.00	0.0117	-22.22	-99
10.00	0.0045	-30.52	-473

Range was ± 20 deg/sec.

+20°F Ambient-Temperature Test

The system was mounted in a temperature chamber along with the oscillating table to provide a cyclic input to the system. The system was soaked overnight at +20°F and then started and allowed to stabilize at normal operating fluid temperature. (It took 30 min. to stabilize.) A performance test was then run. The results are shown in Table VII.

TABLE VII. +20°F AMBIENT ENVIRONMENTAL PERFORMANCE TEST

Frequency (cps)	Gain (in. /deg/sec)	20 Log 6.62 Gain (db)	Phase (deg)
0.02	0.0074	-26.20	+81
0.50	0.0219	-16.78	0
3.00	0.0109	-22.84	-110
10.00	0.0083	-25.20*	-365

*Gain exceeded failure limit; range was ±20 deg/sec.

+100°F Ambient-Temperature Test

The system, mounted in the temperature chamber, was soaked for four hours at 100°F and then started. It reached its stabilized temperature one minute after the system was turned on. Table VIII lists the performance data for this test.

TABLE VIII. +100°F ENVIRONMENTAL PERFORMANCE TEST

Frequency (cps)	Gain (in./deg/sec)	20 log 6.62 Gain (db)	Phase (deg)
0.02	0.0065	-27.34	+83
0.50	0.0220	-16.72	-16
3.00	0.0111	-22.68	-118
10.00	0.0030	-34.06	-347

Range was ± 20 deg/sec.

Post-Environmental Test

A final performance test was performed on the system after the environmental tests. The results are given in Table IX.

TABLE IX. POST-ENVIRONMENTAL PERFORMANCE TEST

Frequency (cps)	Gain (in. /deg/sec)	20 log 6.62 Gain (db)	Phase (deg)
0.02	0.0071	-26.56	+77
0.50	0.0260	-15.30	-16
3.00	0.0124	-21.72	-117
10.00	0.0040	-31.54	-356

Range was ±20 deg/sec.

Closed-Loop Test

The final test performed on the system was a closed-loop test. The UH-1B helicopter's airframe dynamics were simulated on an analog computer. The purpose of the test was to show improved aircraft damping ratio. Data were determined from the sideslip trace on the closed-loop response data and were obtained during simulated wind gust inputs and pilot rudder commands. The overshoot ratio was converted to equivalent second-order damping. Table X lists the overshoot ratio and the damping ratio for free and augumented aircraft during three flight conditions.

Test Results

The system successfully passed all of the performance tests with two exceptions. During the initial previbration test and the +20°F environmental test, the gain at 10 cps exceeded the +5 db limit. An Engineering Variation Authorization No. 68-1032 was written to waive the two parameter variations.

The closed-loop simulation test showed improved aircraft damping from 0.35 to 0.60.

TABLE X. CLOSED-LOOP RESPONSE

Flight Condition	$+\beta$		$-\beta$		$+\theta_T$		$-\theta_T$	
	0.S	ζ	0.S	ζ	0.S	ζ	0.S	ζ
60 Knots - Free	0.290	0.365	0.300	0.360	0.300	0.360	0.280	0.375
Aug.	0.097	0.600	0.100	0.595	0.080	0.630	0.140	0.530
90 Knots - Free	0.320	0.340	0.320	0.340	0.303	0.355	0.303	0.355
Aug.	0.097	0.600	0.090	0.610	0.120	0.560	0.100	0.595
120 Knots - Free	0.320	0.340	0.330	0.330	0.310	0.350	0.290	0.365
Aug.	0.087	0.620	0.080	0.630	0.110	0.575	0.110	0.575

β ~ wind gust step inputs (sideslip angle)
θ_T ~ pilot command tail rotor step input
ζ ~ aircraft damping ratio
0.S ~ percent overshoot

Unclassified
Security Classification

DOCUMENT CONTROL DATA - R & D

(Security classification of title, body of abstract and indexing annotation must be entered when the overall report is classified)

1. ORIGINATING ACTIVITY (Corporate author) Honeywell Inc., Aerospace Division Minneapolis, Minnesota	2a. REPORT SECURITY CLASSIFICATION Unclassified
	2b. GROUP

3. REPORT TITLE
FABRICATION AND FUNCTIONAL TEST OF A FLIGHTWORTHY FLUIDIC YAW DAMPER

4. DESCRIPTIVE NOTES (Type of report and inclusive dates)
Final Report, 28 June 1967 to 28 April 1968

5. AUTHOR(S) (First name, middle initial, last name)
Walter M. Posingies

6. REPORT DATE October 1968	7a. TOTAL NO. OF PAGES 66	7b. NO. OF REFS 0

8a. CONTRACT OR GRANT NO. DAAJ02-67-C-0056	9a. ORIGINATOR'S REPORT NUMBER(S)
b. PROJECT NO. Task 1F121401A14186	USAAVLABS Technical Report 68-62
c.	9b. OTHER REPORT NO(S) (Any other numbers that may be assigned this report)
d.	20885-FR1

10. DISTRIBUTION STATEMENT
This document has been approved for public release and sale; its distribution is unlimited.

11. SUPPLEMENTARY NOTES	12. SPONSORING MILITARY ACTIVITY U.S. Army Aviation Materiel Laboratories Fort Eustis, Virginia

13. ABSTRACT

The objective of this program was to design, fabricate, and perform acceptance tests on a flightworthy fluidic yaw damper system and to provide support to the Bell Helicopter Company during flight evaluation of the system. Control-system characteristics were optimized for the UH-1 series helicopters. This program incorporated significant improvements in the areas of component design, high-pass circuit simplification, noise reduction, and fabrication techniques. Temperature compensation studies illustrated a technique for maintaining a relatively constant rate-sensor scale factor over a wide range of fluid temperatures. Flightworthiness testing demonstrated that the system provided the required transfer function and was suitable for flight test. The flight test (not reported in this document) confirmed that the system was suitable for the helicopter environments and that it would increase the vehicle directional damping ratio from 0.3 to 0.6. Post-flight tests in the laboratory determined the bench performance of the system under several special conditions to which the system had been adjusted during the flight test. This program demonstrated that fluidic systems operating with hydraulic fluid can accurately provide simple control functions. Consistent and trouble-free performance obtained during this development indicates that fluidic systems should be considered for applications which require similar functions.

DD FORM 1 NOV 65 1473 REPLACES DD FORM 1473, 1 JAN 64, WHICH IS OBSOLETE FOR ARMY USE.

Unclassified
Security Classification

Unclassified
Security Classification

14. KEY WORDS	LINK A		LINK B		LINK C	
	ROLE	WT	ROLE	WT	ROLE	WT
Hydraulics						
Fluidics						
Rate Sensor						
Vortex Rate Sensor						
Helicopter Flight-Control Systems						
Flight Controls						
Damper						
Fluid Amplifiers						
High-Pass						
Fluidic Shaping Networks						

Unclassified
Security Classification

10785-68